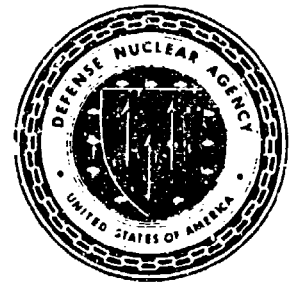


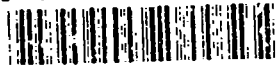
2



Defense Nuclear Agency
Alexandria, VA 22310-3398



AD-A261 397



DNA-TR-92-98

Statistics of Sampled Rician Fading

Roger A. Dana
Mission Research Corporation
P.O. Drawer 719
Santa Barbara, CA 93102-0719

DTIC
ELECTE
MAR 5 1993
S C D

February 1993

Technical Report

CONTRACT No. DNA 001-91-C-0010

Approved for public release;
distribution is unlimited.

93-04679



98-9 4 05T

Destroy this report when it is no longer needed. Do not return to sender.

PLEASE NOTIFY THE DEFENSE NUCLEAR AGENCY,
ATTN: CSTI, 6801 TELEGRAPH ROAD, ALEXANDRIA, VA
22310-3398, IF YOUR ADDRESS IS INCORRECT, IF YOU
WISH IT DELETED FROM THE DISTRIBUTION LIST, OR
IF THE ADDRESSEE IS NO LONGER EMPLOYED BY YOUR
ORGANIZATION.



DISTRIBUTION LIST UPDATE

This mailer is provided to enable DNA to maintain current distribution lists for reports. (We would appreciate your providing the requested information.)

- Add the individual listed to your distribution list.
- Delete the cited organization/individual.
- Change of address.

NOTE:

Please return the mailing label from the document so that any additions, changes, corrections or deletions can be made easily.

NAME: _____

ORGANIZATION: _____

OLD ADDRESS

CURRENT ADDRESS

TELEPHONE NUMBER: () _____

DNA PUBLICATION NUMBER/TITLE

CHANGES/DELETIONS/ADDITIONS, etc.)

(Attach Sheet if more Space is Required)

DNA OR OTHER GOVERNMENT CONTRACT NUMBER: _____

CERTIFICATION OF NEED-TO-KNOW BY GOVERNMENT SPONSOR (if other than DNA): _____

SPONSORING ORGANIZATION: _____

CONTRACTING OFFICER OR REPRESENTATIVE: _____

SIGNATURE: _____

CUT HERE AND RETURN



DEFENSE NUCLEAR AGENCY
ATTN: TITL
6801 TELEGRAPH ROAD
ALEXANDRIA, VA 22310-3398

DEFENSE NUCLEAR AGENCY
ATTN: TITL
6801 TELEGRAPH ROAD
ALEXANDRIA, VA 22310-3398

REPORT DOCUMENTATION PAGE

FORM APPROVED
OMB NO. 0704-0182

Public reporting burden for this collection of information is estimated to average 1 hour per response, including the time for reviewing the instructions, searching existing data sources, gathering and maintaining the data needed, and completing and reviewing the collection of information. Send comments regarding this burden estimate or any other aspect of the collection of information, including suggestions for reducing this burden, to Washington Headquarters Services, Directorate for Information Operations and Reports, 1215 Jefferson Davis Highway, Suite 1204, Arlington, VA 22202-4302, and to the Office of Management and Budget, Paperwork Reduction Project (0704-0188), Washington, DC, 20503.

| | | | | |
|---|--|---|---|--|
| 1. AGENCY USE ONLY (Leave blank) | | 2. REPORT DATE 930201 | 3. REPORT TYPE AND DATES COVERED Technical 920101 - 920631 | |
| 4. TITLE AND SUBTITLE Statistics of Sampled Rician Fading | | | 5. FUNDING NUMBERS C - DNA 001-91-C-0010 PE - 62715H PR - RB TA - RB WU - DH303230 | |
| 6. AUTHOR(s) Roger A. Dana | | | 8. PERFORMING ORGANIZATION REPORT NUMBER MRC-R-1410 | |
| 7. PERFORMING ORGANIZATION NAME(S) AND ADDRESS(ES) Mission Research Corporation P.O. Drawer 719 Santa Barbara, CA 93102-0719 | | | 10. SPONSORING/MONITORING AGENCY REPORT NUMBER DNA-TR-92-98 | |
| 9. SPONSORING/MONITORING AGENCY NAME(S) AND ADDRESS(ES) Defense Nuclear Agency 6801 Telegraph Road Alexandria, VA 22310-3398 RAAE/Ullrich | | | 11. SUPPLEMENTARY NOTES This work was sponsored by the Defense Nuclear Agency under RDT&E RMC Code B4652D RB RB 10145 RAAE 3208A 25904D. | |
| 12a. DISTRIBUTION/AVAILABILITY STATEMENT Approved for public release; distribution is unlimited. | | | 12b. DISTRIBUTION CODE | |
| 13. ABSTRACT (Maximum 200 words) Realizations of the channel impulse response function generated with Rician amplitude statistics have been used for many years to evaluate system performance in the regime between full Rayleigh fading and ambient non-fading conditions. While it is well known that Rician distributed realizations fail to match observed phase fluctuations, Rician statistics provide a worst case description of the occurrence of deep fades. Thus the use of Rician statistics is attractive in slow fading situations where system performance has been rendered insensitive to phase variations. The purposes of this report are to provide new information on the temporal statistics of Rician fading (mean fade duration and separation) and to determine sampling requirements on realizations of the channel impulse response function with Rician amplitude statistics. It is found that 400 decorrelation time (τ_0) realizations generated with 10 samples per τ_0 and sampled at $\tau_0/40$ accurately reproduce the temporal statistics of Rician fading. | | | | |
| 14. SUBJECT TERMS Temporal Statistics Scintillation Rician Fading Rayleigh Fading | | | 15. NUMBER OF PAGES 60 | |
| | | | 16. PRICE CODE | |
| 17. Security CLASSIFICATION OF REPORT UNCLASSIFIED | 18. Security CLASSIFICATION OF THIS PAGE UNCLASSIFIED | 19. Security CLASSIFICATION OF ABSTRACT UNCLASSIFIED | 20. LIMITATION OF ABSTRACT SAR | |

UNCLASSIFIED

SECURITY CLASSIFICATION OF THIS PAGE

CLASSIFIED BY:

N/A Since Unclassified.

DECLASSIFY ON:

N/A Since Unclassified.

UNCLASSIFIED

SECURITY CLASSIFICATION OF THIS PAGE

CONVERSION TABLE

Conversion factors for U.S. Customary to metric (SI) units of measurement

MULTIPLY $\xrightarrow{\hspace{2cm}}$ BY $\xrightarrow{\hspace{2cm}}$ TO GET
 TO GET $\xleftarrow{\hspace{2cm}}$ BY $\xleftarrow{\hspace{2cm}}$ DIVIDE

| | | |
|--|----------------------------|--|
| angstrom | 1.000000 x E -10 | meters (m) |
| atmosphere (normal) | 1.01325 x E +2 | kilo pascal (kPa) |
| bar | 1.000000 x E +2 | kilo pascal (kPa) |
| barn | 1.000000 x E -28 | meter ² (m ²) |
| British thermal unit (thermochemical) | 1.054350 x E +3 | joule (J) |
| calorie (thermochemical) | 4.184000 | joule (J) |
| cal (thermochemical) / cm ² | 4.184000 x E -2 | mega joule/m ² (MJ/m ²) |
| curie | 3.700000 x E +1 | *giga becquerel (GBq) |
| degree (angle) | 1.745329 x E -2 | radian (rad) |
| degree Fahrenheit | $t_K = (t_F + 459.67)/1.8$ | degree kelvin (K) |
| electron volt | 1.60219 x E -19 | joule (J) |
| erg | 1.000000 x E -7 | joule (J) |
| erg/second | 1.000000 x E -7 | watt (W) |
| foot | 3.048000 x E -1 | meter (m) |
| foot-pound-force | 1.355818 | joule (J) |
| gallon (U.S. liquid) | 3.785412 x E -3 | meter ³ (m ³) |
| inch | 2.540000 x E -2 | meter (m) |
| jerk | 1.000000 x E +9 | joule (J) |
| joule/kilogram (J/kg) (radiation dose absorbed) | 1.000000 | Gray (Gy) |
| kilotons | 4.183 | terajoules |
| kip (1000 lbf) | 4.448222 x E +3 | newton (N) |
| kip/inch ² (ksi) | 6.894757 x E +3 | kilo pascal (kPa) |
| ktap | 1.000000 x E +2 | newton-second/m ² (N-s/m ²) |
| micron | 1.000000 x E -6 | meter (m) |
| mil | 2.540000 x E -5 | meter (m) |
| mile (international) | 1.609344 x E +3 | meter (m) |
| ounce | 2.834952 x E -2 | kilogram (kg) |
| pound-force (lbs avoirdupois) | 4.448222 | newton (N) |
| pound-force inch | 1.129848 x E -1 | newton-meter (N-m) |
| pound-force/inch | 1.751268 x E +2 | newton/meter (N/m) |
| pound-force/foot ² | 4.788026 x E -2 | kilo pascal (kPa) |
| pound-force/inch ² (psi) | 6.894757 | kilo pascal (kPa) |
| pound-mass (lbm avoirdupois) | 4.535924 x E -1 | kilogram (kg) |
| pound-mass-foot ² (moment of inertia) | 4.214011 x E -2 | kilogram-meter ² (kg-m ²) |
| pound-mass/foot ³ | 1.601846 x E +1 | kilogram/meter ³ (kg/m ³) |
| rad (radiation dose absorbed) | 1.000000 x E -2 | **Gray (Gy) |
| roentgen | 2.579760 x E -4 | coulomb/kilogram (C/kg) |
| shake | 1.000000 x E -8 | second (s) |
| slug | 1.459390 x E +1 | kilogram (kg) |
| torr (mm Hg, 0° C) | 1.333220 x E -1 | kilo pascal (kPa) |

*The becquerel (Bq) is the SI unit of radioactivity; 1 Bq = 1 event/s.

**The Gray (Gy) is the SI unit of absorbed radiation.

DTIC QUALITY INSPECTED 1

| | |
|--------------------|-------------------------------------|
| Accession For | |
| NTIS CRA&I | <input checked="" type="checkbox"/> |
| DTIC TAB | <input type="checkbox"/> |
| Unannounced | <input type="checkbox"/> |
| Justification | |
| By | |
| Distribution / | |
| Availability Codes | |
| Avail and/or | |
| A-1 | |

TABLE OF CONTENTS

| Section | Page |
|--|------|
| CONVERSION TABLE | iii |
| LIST OF ILLUSTRATIONS | v |
| 1 INTRODUCTION..... | 1 |
| 1.1 Rician Statistics..... | 2 |
| 1.2 Sampling Statistics | 3 |
| 2 TEMPORAL STATISTICS OF RICIAN FADING | 6 |
| 2.1 First Order Statistics..... | 6 |
| 2.2 DBPSK Example | 9 |
| 2.3 Second Order Statistics | 11 |
| 2.4 Temporal Statistics..... | 14 |
| 3 SAMPLED RICIAN FADING..... | 20 |
| 3.1 Measured First Order Statistics..... | 21 |
| 3.2 Measured Second Order Statistics | 25 |
| 4 LIST OF REFERENCES | 32 |
| | |
| Appendices | Page |
| A REALIZATIONS OF RICIAN FADING..... | A-1 |
| B JOINT PROBABILITY DENSITY FUNCTION $f(a,a')$ | B-1 |
| C VARIATION IN THE MEASUREMENT OF MEAN POWER..... | C-1 |

LIST OF ILLUSTRATIONS

| Figure | | Page |
|--------|--|------|
| 1 | Rician amplitude probability density function..... | 8 |
| 2 | Rician phase probability density function..... | 8 |
| 3 | Cumulative distribution of Rician fading | 10 |
| 4 | DBPSK symbol error rate for Rician fading..... | 11 |
| 5 | Realizations of Rayleigh fading with Gaussian, f^{-6} , and f^{-4} Doppler spectra... 13 | |
| 6 | Realizations of Rician fading with f^{-4} Doppler spectra and scintillation indices of 1.0, 0.75, 0.5, and 0.25..... | 15 |
| 7 | Mean number of level crossings per τ_0 for several scintillation indices | 17 |
| 8 | Mean duration of Rician distributed fades..... | 18 |
| 9 | Mean separation of Rician distributed fades | 19 |
| 10 | Amplitude moments of the Rician distribution..... | 22 |
| 11 | Log amplitude moments of the Rician distribution..... | 23 |
| 12 | Measured cumulative distribution for $S_4 = 1.0$ | 26 |
| 13 | Measured cumulative distribution for $S_4 = 0.75$ | 26 |
| 14 | Measured cumulative distribution for $S_4 = 0.5$ | 27 |
| 15 | Measured cumulative distribution for $S_4 = 0.25$ | 27 |
| 16a | Measured mean fade duration for $S_4 = 1.0$ | 28 |
| 16b | Measured mean fade separation for $S_4 = 1.0$ | 28 |
| 17a | Measured mean fade duration for $S_4 = 0.75$ | 29 |
| 17b | Measured mean fade separation for $S_4 = 0.75$ | 29 |
| 18a | Measured mean fade duration for $S_4 = 0.5$ | 30 |
| 18b | Measured mean fade separation for $S_4 = 0.5$ | 30 |
| 19a | Measured mean fade duration for $S_4 = 0.25$ | 31 |
| 19b | Measured mean fade separation for $S_4 = 0.25$ | 31 |

LIST OF ILLUSTRATIONS (Continued)

| Figure | | Page |
|--------|-------------------------------|------|
| 20 | Power measurement error | C-4 |

SECTION 1 INTRODUCTION

Design, evaluation, and testing of trans-ionospheric radio frequency (RF) communication systems require high fidelity channel models and detailed knowledge of fading channel statistics. Such models can be used to construct realizations of the received signal for use in digital simulations or hardware channel simulators. During the design process, knowledge of channel fading statistics is used to develop power requirements, size interleavers, and assess performance, for example.

The design goal for a truly robust trans-ionospheric communications system is to achieve performance that is acceptable over the entire range of possible fading conditions from fast, frequency selective, Rayleigh fading to slow, flat fading including the regime between Rayleigh fading and a non-fading channel. While considerable effort has been expended in the nuclear effects community over the past three decades to characterize the Rayleigh fading channel and to develop Rayleigh fading mitigation techniques, somewhat less effort has been directed at robust design and performance in non-Rayleigh fading. One reason for this is that if a system is properly designed to successfully operate over the full range of Rayleigh fading, then it is generally assumed that it will also perform well in non-Rayleigh fading.

There are situations, however, where this assumption may not be valid. For example, the performance of many systems is degraded in slow Rayleigh fading where long, deep fades can cause tracking loops to lose lock on the received signal. A natural question to ask is the following: What happens to receiver performance in slightly non-Rayleigh fading where the channel coherence time may be longer than under Rayleigh fading? Does performance degrade further because the fades may be longer or does it improve because the fades are generally not as deep?

Effects of non-Rayleigh fading are also important in determining the performance of systems that have not been designed to operate under highly disturbed ionospheric conditions. An obvious question is: Will these systems perform adequately under weakly disturbed (either man-made or naturally occurring) ionospheric conditions? This question should be addressed before effort is spent to needlessly upgrade communications systems that may already perform adequately in weak scintillation or before fragile communications systems unexpectedly fail.

The purpose of this report and a companion report [Dana, 1992b] is to extend existing Defense Nuclear Agency (DNA) channel models to include the non-Rayleigh fading regime. Ideally these models will then cover *all* possible fading conditions, from fast, frequency selective fading caused by a highly disturbed ionosphere to naturally occurring slow, non-Rayleigh fading. Such models are needed for the design, analysis, and testing of existing and new communications systems.

The problem with a general-purpose channel model is that the statistics of non-Rayleigh fading are not described by any single mathematical expression, as is the case

for Rayleigh fading. Thus it is the intent of the companion report, *Temporal Statistics of Non-Rayleigh Fading*, to demonstrate that Rician statistics provide a reasonable worst case channel model in this regime. In this report, temporal statistics (i.e., mean fade duration and separation) of Rician fading are derived. These statistics are then used to demonstrate that realizations of sampled Rician fading can be generated with the desired statistics. In *Dana [1992b]* the temporal statistics of non-Rayleigh fading are analyzed, and it is shown that Rician statistics may provide a reasonable worst case for the cumulative distribution, mean fade duration, and mean fade separation.

1.1 RICIAN STATISTICS.

Realizations of the channel impulse response function generated with Rician amplitude statistics [*Rice, 1948*] have been used for many years to evaluate system performance in the regime between full Rayleigh fading and ambient non-fading conditions. This approach is often used because it is easy to generate a realization of Rician fading from a realization of Rayleigh fading by simply adding a constant component to the complex impulse response function, appropriately re-normalized to maintain constant power.

However researchers in the area of ionospheric physics (see, for example, *Fremouw, Livingston, and Miller [1980]*; *Rino and Fremouw [1973]*; *Rino, Livingston, and Whitney [1976]*; and *Whitney, et al. [1972]*) have suggested that Nakagami-m, generalized Gaussian, or log-normal distributions may more accurately describe the observed amplitude distribution of RF scintillation caused by the ambient ionosphere.

None of these distributions or the Rician distribution adequately describe the observed phase fluctuations of non-Rayleigh fading. Indeed, the Nakagami-m and log-normal distributions *only* describe amplitude fluctuations. Often two-component models, one for amplitude and another for phase, are used to describe the statistics of observed trans-ionospheric signals (see, for example, *Wittwer [1980]*). However, such two-component models *may not* accurately reproduce observed amplitude-phase correlation of non-Rayleigh fading [*Fremouw, Livingston, and Miller, 1980*].

Two important points should be noted about proper design of robust trans-ionospheric communications systems. First, performance should be insensitive to the random phase fluctuations encountered on a the link. Second, it is important that the performance is insensitive to the differences between the various fading distributions. All are possible, so the system should be designed to perform against the reasonable worst case. If phase fluctuations are important, then separate Total Electron Content (TEC) dynamics models are available to stress the system [*Wittwer, 1980*; *Frasier, 1988*].

Recently *De Raad and Grover [1990]* undertook a theoretical study of the amplitude statistics of non-Rayleigh fading for a wide range of ionospheric conditions. They conclude that (1) *none* of these models is reliable in general; (2) the actual amplitude distribution has a strong dependence on the power spectrum of the scattering

ionospheric structure as well as the Fresnel length; and (3) Rician amplitude statistics provide a useful "worst case" description of the occurrence of deep fades.

Multiple phase screen (MPS) techniques (e.g., *Knepp* [1983]; *De Raad and Grover* [1990]) can be used to generate realizations of the channel impulse response function that represent direct solutions to Maxwell's equations. These higher fidelity realizations exhibit a large range of amplitude and phase fluctuations under non-Rayleigh fading conditions. However *De Raad and Grover* [1990] correctly observe that the uncertainty in the validity of MPS realizations has been shifted from the amplitude and phase distributions to the statistical description of the scattering medium.

Still, the temptation persists to use Rician fading realizations for non-Rayleigh fading. They are easy to generate from Rayleigh fading realizations, and they contain phase fluctuations (albeit fluctuations that differ significantly from observations). By comparison with MPS realizations of non-Rayleigh fading, *De Raad and Grover* [1990] show that Rician amplitude statistics represent a reasonable worst case for the observed cumulative distribution of fades, and *Dana* [1992b] shows that Rician temporal statistics also represent a reasonable worst case for the observed mean fade duration and separation.

The purpose of this report is to provide further information on the temporal statistics (mean fade duration and separation) of Rician fading and to define sampling requirements of Rician realizations of the channel impulse response function. These analytic results are compared to measured values from a representative set of MPS realizations in *Dana* [1992b] where utility of Rician temporal statistics in bounding the observed range of fade durations and separations in MPS realizations is demonstrated.

1.2 SAMPLING STATISTICS.

The original version of this report [*Dana* 1988] was intended to address three questions that arise during simulation or hardware testing activities of communications links under Rayleigh fading conditions: (1) How many decorrelation times (τ_0) per realization of the channel impulse response function are necessary? (2) How many samples per decorrelation time are necessary? (3) How should interpolation be done between samples? This report re-addresses these questions for the more general case of Rician fading, and more completely addresses an additional question: (4) What is the expected variation in measured parameters of a realization?

The fourth question can arise in at least two situations. The efficacy of a realization of the channel impulse response function may be in question, or it may be necessary to validate a realization for use in hardware testing. An approach used by the author to validate realizations is to measure key parameters, such as mean power, amplitude moments, decorrelation time, and number of samples per decorrelation time. These measured parameters should agree with ensemble values to within some tolerance. The question is: What tolerance? *Dana* [1991] partially addresses this question. This report incorporates some recent findings on the expected tolerance of measured realization parameters.

The first three questions are answered in part in the DNA signal specification for nuclear scintillation [Wittwer, 1980] which requires a minimum of 100 decorrelation times per realization and 10 samples per decorrelation time. However considerable statistical variation in receiver performance is seen when the minimum realization length is used. This is particularly true of links that have large power margins and are susceptible to only the deepest fades. Of course the best answer to these questions is to measure link performance with realizations of increasing length and resolution until the statistical variation in the results from one realization to the next is acceptable. Unfortunately the luxury of doing this analysis ordinarily does not exist.

The next higher level of analysis of these questions is to look at the statistics of the realizations. This is the approach that will be taken in this report. The first order statistics of realizations are measured by calculating amplitude moments and the cumulative distribution and comparing these to ensemble values for Rayleigh fading. The second order statistics of the realizations are measured by calculating the mean duration and separation of fades.

In general, the received signal may be written as the convolution of the channel impulse response function $h(t, \tau)$ with the transmitted modulation $m(t)$:

$$u(t) = \int_0^{\infty} h(t, \tau) m(t-\tau) d\tau \quad (1.1)$$

In either software link simulations or in hardware channel simulator, Equation 1.1 can be implemented as a tapped delay line:

$$u(t) = \sum_{j=0}^{N_{\tau}-1} h(t, j\Delta\tau) m(t-j\Delta\tau) \Delta\tau \quad (1.2)$$

where N_{τ} is number of taps on the delay line; $\Delta\tau$ is the delay spacing of the delay line; and $h(t, j\Delta\tau)$ is the time varying complex weight of the j^{th} tap. In a software simulation of link performance time will also be discretely sampled (i.e., $t = k\Delta t$).

Under Rayleigh fading conditions $h(t, \tau)$ is a complex, zero mean, normally distributed random variable and thus has a Rayleigh amplitude distribution. It then follows from Equation 1.2 that $u(t)$ is also a complex, zero mean, normally distributed random variable with a Rayleigh amplitude distribution.

A complete analysis of the first three questions would consider the sampling requirements for each delay of the discrete impulse response function $h(k\Delta t, j\Delta\tau)$. However this is beyond the scope of this report. Therefore sampling requirements on the flat fading impulse response function $h(k\Delta t)$, where

will be addressed in this report. The sampling requirements for $h(k\Delta t)$ will give some indication of the sampling requirements for the frequency selective impulse response function $h(k\Delta t, j\Delta \tau)$. Perhaps this should be stated another way: Sampling that is inadequate for $h(k\Delta t)$ will surely be inadequate for $h(k\Delta t, j\Delta \tau)$. Thus it is the intent of this report to define adequate sampling for $h(k\Delta t)$ and to infer adequate sampling requirements for each delay of $h(k\Delta t, j\Delta \tau)$.

SECTION 2 TEMPORAL STATISTICS OF RICIAN FADING

This section is a generalization of well-known results from the classical work of Rice [1948, 1954, 1958] on the first and second order statistics of Rayleigh fading. To the author's knowledge, the extension of Rice's results on temporal statistics to non-Rayleigh fading is new.

2.1 FIRST ORDER STATISTICS.

Under strong scattering conditions, the electric field incident on the plane of the receiver is the summation of many waves propagating in slightly different directions about the line-of-sight. Under the central limit theorem of statistics, the two orthogonal components of the electric field must then be zero-mean, normally distributed random variables. It is assumed that the two orthogonal components are also independent. The complex narrow-band envelope of the electric field undergoing Rayleigh fading may be then represented as

$$E(t) = x(t) + i y(t)$$

where x and y are independent and normally distributed with zero mean and standard deviation σ . The carrier frequency term, $\exp(i\omega t)$, has been neglected in this expression. Thus $E(t)$ may be thought of as the output voltage of a down-converter where $x(t)$ is the in-phase component and $y(t)$ is the quadrature-phase component.

Under mild to weak scattering conditions, a *model* of the electric field is a specular component plus a normally distributed random component. The electric field is then written as

$$E(t) = [x(t) + r \cos \vartheta] + i [y(t) + r \sin \vartheta]$$

where r is the constant component and ϑ is a constant phase. Clearly Rayleigh fading corresponds to the case where r is zero.

Rice [1948] was the first to show that the probability density function of the amplitude of $E(t)$,

$$a(t) = \sqrt{E(t)E^*(t)}$$

has the probability density function:

$$f(a) = \frac{a}{\sigma^2} \exp\left[-\frac{a^2 + r^2}{2\sigma^2}\right] I_0\left[\frac{ar}{\sigma^2}\right] \quad (2.1)$$

where $I_0(\cdot)$ is the modified Bessel function.

For the mean power of of the electric field,

$$P_0 = \langle a^2 \rangle = 2\sigma^2 + r^2 ,$$

to be constant, the power of the fluctuating component, $2\sigma^2$, must be reduced as the power of the specular component, r^2 , is increased. To keep track of this in a consistent manner both are written in terms of the scintillation index S_4 , where

$$S_4 = \left[\frac{\langle a^4 \rangle - \langle a^2 \rangle^2}{\langle a^2 \rangle^2} \right]^{\frac{1}{2}}.$$

The powers of the two components are then:

$$2\sigma^2 = P_0(1-R)$$

$$r^2 = P_0R$$

where the "Rician" index R is

$$R = \sqrt{1 - S_4^2}.$$

The Rician index is the fraction of the total power that is in the constant component.

Upon writing σ and r in terms of R , Equation 2.1 becomes

$$f(a) = \frac{2a}{P_0(1-R)} \exp\left[-\frac{a^2/P_0 + R}{1-R}\right] I_0\left[\frac{2\sqrt{Ra^2/P_0}}{1-R}\right].$$

The corresponding phase θ of the electric field is

$$\theta = \tan^{-1} \left[\frac{x(t) + r \cos \vartheta}{y(t) + r \sin \vartheta} \right].$$

The probability density function of the phase is

$$f(\theta) = \frac{1}{2\pi} \exp\left[-\frac{R}{1-R}\right] + \frac{1}{2} \left[\frac{R}{\pi(1-R)} \right]^{\frac{1}{2}} \cos(\theta - \vartheta) \times \\ \exp\left\{ -\frac{R[1 - \cos(\theta - \vartheta)]}{1-R} \right\} \left\{ 1 + \operatorname{erf} \left[\left(\frac{R}{1-R} \right)^{\frac{1}{2}} \cos(\theta - \vartheta) \right] \right\}$$

where $\operatorname{erf}(\cdot)$ is the error function. The probability density function of phase is just $1/2\pi$ when the scintillation index is unity ($R=0$), as it should be for Rayleigh fading.

These two probability density functions are plotted in Figures 1 and 2 for several values of the scintillation index. Amplitude in Figure 1 is $a\sqrt{P_0}$, and phase in Figure 2 is the quantity $\theta - \vartheta$. The solid line curves in both figures are the Rayleigh limits. As expected, both functions approach delta functions as the scintillation index approaches zero.

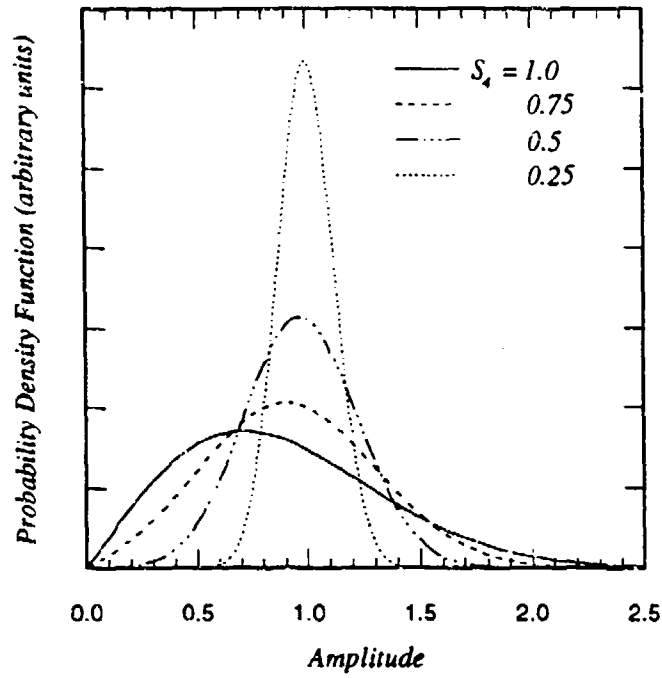


Figure 1. Rician amplitude probability density function.

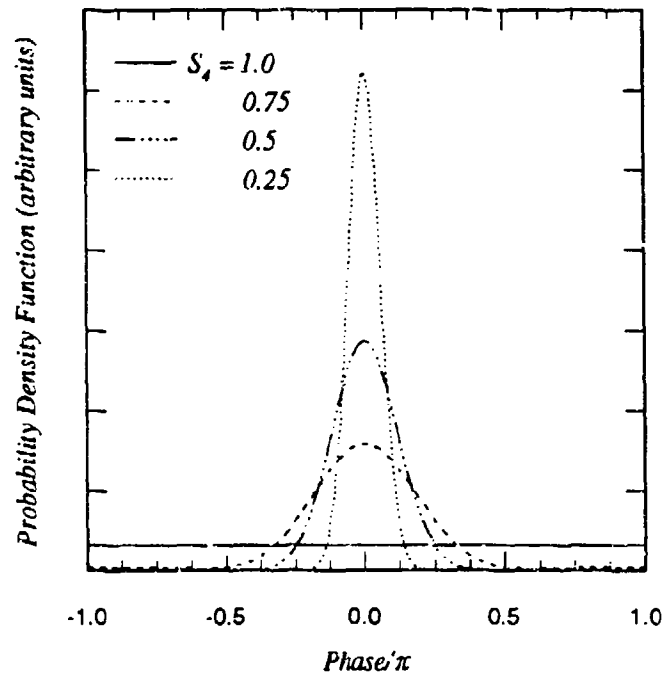


Figure 2. Rician phase probability density function.

The cumulative distribution of the power P ($P = a^2$), which is equal to the probability that the instantaneous power is less than or equal to P , is given by

$$F(P) = \int_0^{\sqrt{P}} f(a) da = \exp\left[-\frac{R}{1-R}\right] \sum_{n=0}^{\infty} \frac{1}{\Gamma^2(n+1)} \left[\frac{R}{1-R}\right]^n \gamma\left[n+1, \frac{P/P_0}{1-R}\right] \quad (2.2)$$

where $\gamma(n,x)$ is the incomplete gamma function and $\Gamma(n+1) = n!$ is the gamma function. The summation is obtained by expanding the Bessel function in a power series and then performing the integration term-by-term. This form of Marcum's Q function [Marcum, 1948] is easily evaluated for values of R that are not too close to unity. In particular Equation 2.2 converges slowly for values of S_4 less than 0.25, corresponding to R values greater than 0.96.

For the Rayleigh case the cumulative distribution is exponential:

$$F(P) = 1 - \exp\left[-\frac{P}{P_0}\right] \quad (S_4 = 1)$$

The Rician cumulative distribution function is plotted in Figure 3 versus the ratio P/P_0 for several values of the scintillation index. For values of the scintillation index between 0.75 and unity the Rician cumulative distribution is close to the Rayleigh curve. As the scintillation index is reduced from about 0.75 to 0.5, the probability of deep fades is significantly reduced. It is noteworthy that case where the power of the specular and fluctuating components are equal corresponds to an S_4 value of $\sqrt{3/4}$ ($S_4 = 0.866$). Thus a Rician cumulative distribution does not deviate significantly from a Rayleigh distribution until more than half of the power is in the constant component. Of course the performance a receiver may be quite sensitive to the existence of a specular component.

2.2 DBPSK EXAMPLE.

An easily calculated example of the effects of Rician fading is the differentially coherent binary phase-shift keying (DBPSK) symbol error rate. The well known DBPSK symbol error rate for an additive white Gaussian noise (AWGN) channel is

$$P_{SE} = \frac{1}{2} e^{-\gamma P} \quad (\text{AWGN Channel}) \quad (2.3)$$

where γ is the symbol energy-to-noise density ratio and P is unity for this channel. In a Rician fading channel this error rate must be averaged over the probability density function of the fading power $P = a^2$:

$$\langle P_{SE} \rangle = \int_0^{\infty} \frac{1}{2} \exp[-\gamma a^2] f(a) da$$

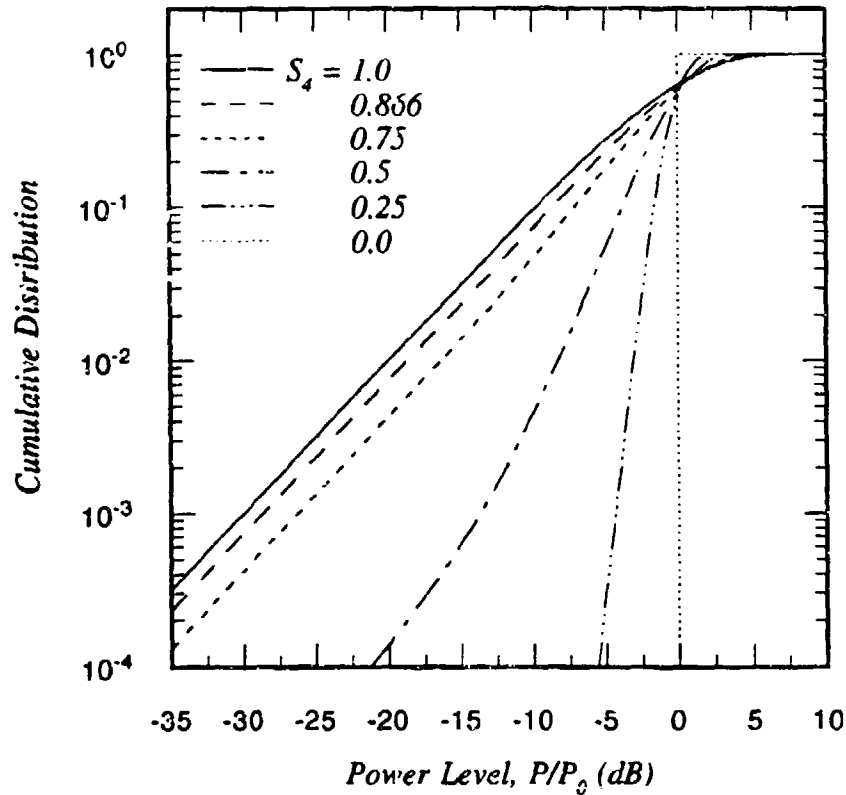


Figure 3. Cumulative distribution of Rician fading.

This equation is easily evaluated using Equation 2.1 with the result:

$$\langle P_{SE} \rangle = \frac{1}{2[1+(1-R)\gamma]} \exp\left[\frac{-R\gamma}{1+(1-R)\gamma}\right] \quad (\text{Rician Channel}) .$$

When R is unity, corresponding to the non-fading case, this expression reduces to Equation 2.3. When R is zero, corresponding to full Rayleigh fading, it reduces to the well-known form:

$$\langle P_{SE} \rangle = \frac{1}{2[1+\gamma]} \quad (\text{Rayleigh Channel}) .$$

Plots of the Rician channel DBPSK error rates for several values of the scintillation index are in Figure 4. As one might expect from examining the cumulative distribution, the DBPSK symbol error rate for a Rician fading channel is close to the full Rayleigh fading channel error rate when the scintillation index is larger than about 0.75, and is close to the AWGN error rate when the scintillation index is less than about 0.25. Thus for DBPSK the most interesting values of scintillation index, excluding 1 and 0, are between 0.75 and 0.25.

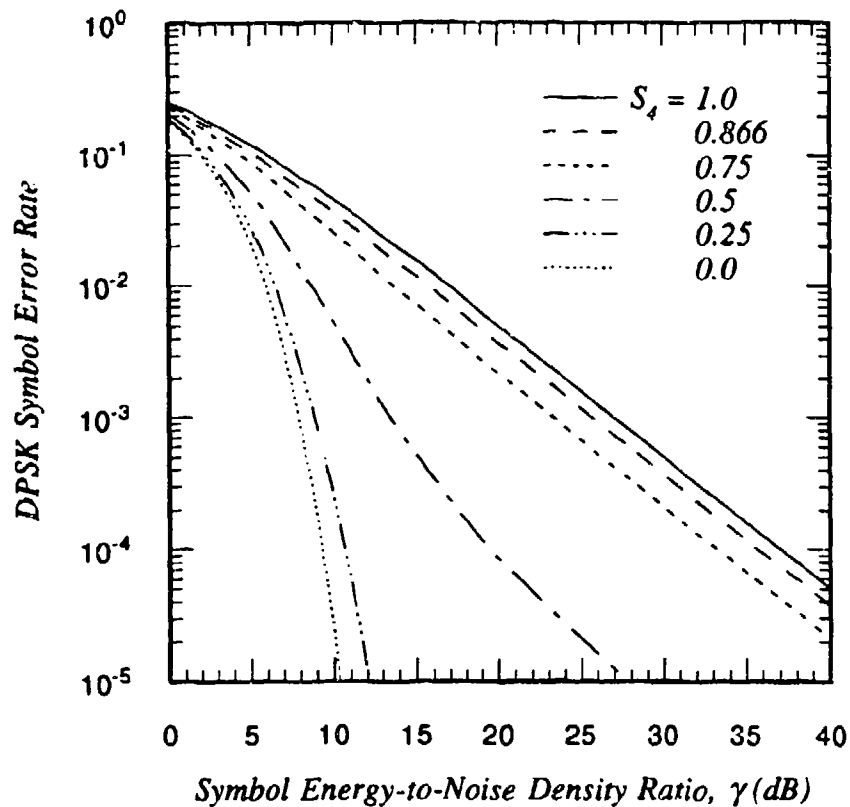


Figure 4. DBPSK symbol error rate for Rician fading.

2.3 SECOND ORDER STATISTICS.

The fading rate is determined by the second order statistics of the fluctuating part of the electric field. The autocovariance of the electric field is, in general,

$$\langle [E(t) - E_0][E^*(t+\tau) - E_0^*] \rangle = \langle x(t)x(t+\tau) \rangle + \langle y(t)y(t+\tau) \rangle = 2\sigma^2 \rho(\tau)$$

where

$$E_0 = r \cos \vartheta + i r \sin \vartheta .$$

There are two limiting forms for the correlation function $\rho(\tau)$. Under strongly disturbed scattering conditions that occur at early times or at the center of the disturbed region, $\rho(\tau)$ has the Gaussian form

$$\rho(\tau) = \exp \left[-\frac{\tau^2}{\tau_0^2} \right]$$

where τ_0 , the decorrelation time of the electric field, is defined as the e folding point of the autocorrelation function [$\rho(\tau_0) = e^{-1}$]. The corresponding Doppler spectrum of the temporal fluctuations is

$$S(\omega_D) = \int_{-\infty}^{\infty} \exp(-i\omega_D \tau) \rho(\tau) d\tau = \sqrt{\pi} \tau_0 \exp\left[-\frac{\tau_0^2 \omega_D^2}{4}\right]$$

which also has the Gaussian form. Under less disturbed conditions, the correlation function is usually assumed to have the form

$$\rho(\tau) = \left[1 + \frac{\alpha_4 |\tau|}{\tau_0}\right] \exp\left[-\frac{\alpha_4 |\tau|}{\tau_0}\right]$$

where the parameter α_4 ($\alpha_4 = 2.146193$) is determined by the condition that $\rho(\tau_0) = e^{-1}$. The corresponding Doppler spectrum has the form commonly referred to as an f^{-4} spectrum:

$$S(\omega_D) = \frac{4\tau_0}{\alpha_4} \frac{1}{[1 + (\tau_0 \omega_D / \alpha_4)^2]^2}$$

A third Doppler spectrum is used for real-time frequency selective channel models [Dana 1992a]. This f^{-5} spectrum has the functional form

$$S(\omega_D) = \frac{16\tau_0}{3\alpha_6} \frac{1}{[1 + (\tau_0 \omega_D / \alpha_6)^2]^3}$$

where the normalization of $S(\omega_D)$ is chosen so that $\rho(0)$ is unity. The corresponding correlation function is

$$\rho(\tau) = \left[1 + \frac{\alpha_6 |\tau|}{\tau_0} + \frac{(\alpha_6 \tau)^2}{3\tau_0^2}\right] \exp\left[-\frac{\alpha_6 |\tau|}{\tau_0}\right]$$

where $\alpha_6 = 2.904630$ results from setting $\rho(\tau_0) = e^{-1}$.

A comparison of Rayleigh fading realizations ($S_4 = 1$) of the impulse response function with f^{-4} , f^{-6} , and Gaussian Doppler spectra is shown in Figure 5 where realization power in decibels (dB) is plotted versus time/ τ_0 . These realizations were generated from the same set of random numbers, as described in Appendix A, so there is correlation in the features seen in the three frames. The f^{-4} realization in the bottom frame has the most spiky appearance because it has more energy at high Doppler frequencies. The three realizations have similar low frequency behavior, and fades in the realizations follow each other quite closely. The difference between the realizations is the high frequency jitter of the f^{-4} and f^{-5} realizations about the more smoothly varying Gaussian one. The significance of this on the temporal statistics of the fades will become apparent later.

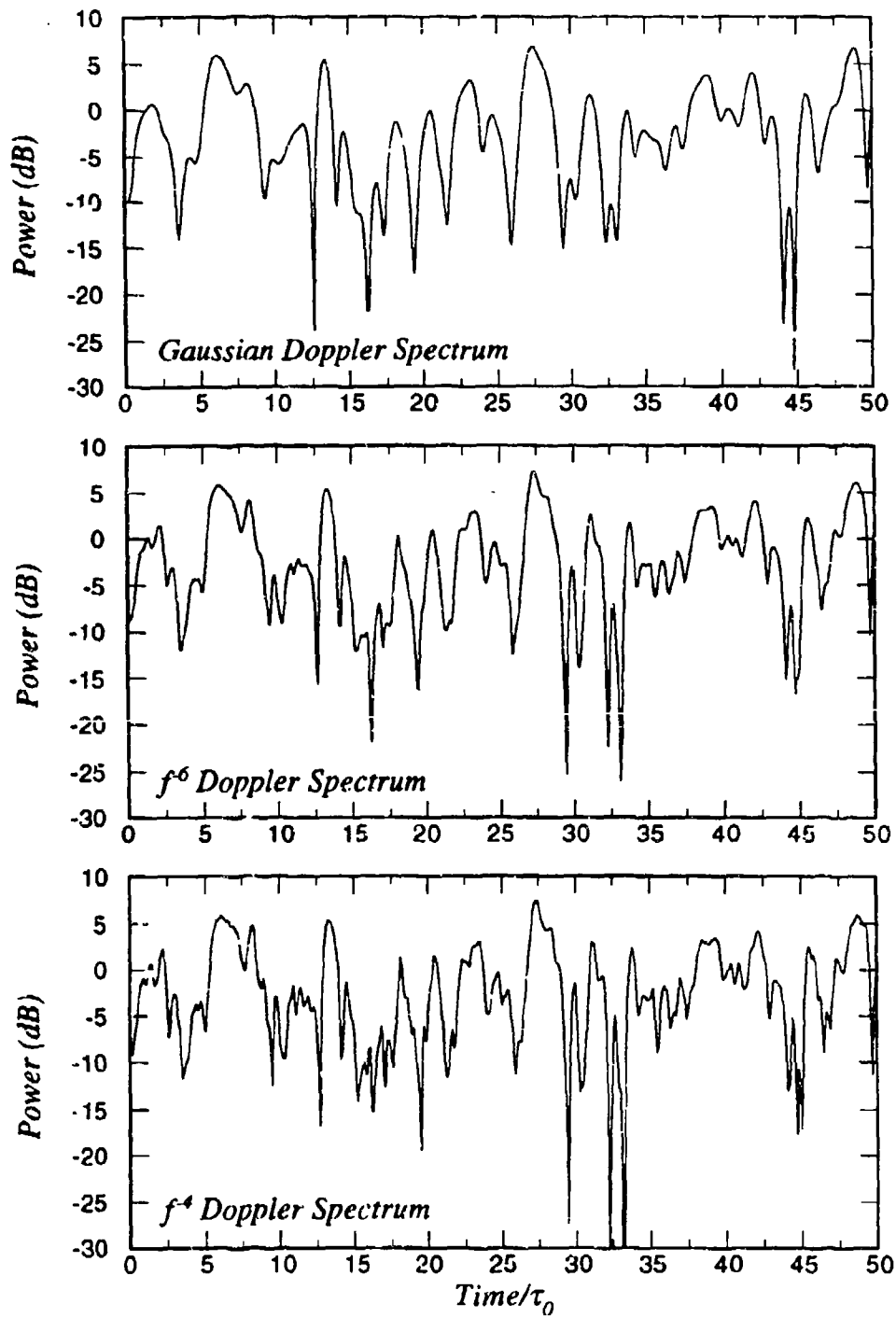


Figure 5. Realizations of Rayleigh fading with Gaussian, f^{-6} , and f^{-4} Doppler spectra.

A comparison of Rician fading realizations of the impulse response function with Doppler spectra and scintillation indices of 1.0, 0.75, 0.5 and 0.25 is shown in Figure 6. Again these realizations were generated from the same set of random numbers, so there is correlation in the features seen in all four plots. As expected, the Rayleigh fading realization in the top frame (reproduced from the bottom frame of Figure 3) has the deepest fades and the largest flares. As the scintillation index is reduced, the deep fades fill in and the power in flares above 0 dB is reduced. It is interesting that as the scintillation index decreases, fades at a given level appear to get longer. This phenomenon is shown theoretically for Rician fading in the developments below.

2.4 TEMPORAL STATISTICS.

The mean duration and separation of fades below an arbitrary power level P and that of flares above P , are calculated from the mean number $\langle N(P,T) \rangle$ of crossings of the level P in the time interval T .

The probability that the amplitude a crosses the level $l = \sqrt{P}$ in the time interval t to $t+dt$ with a positive derivative is equal to the probability that $a' > 0$ and that $l - a' dt < a < l$. This probability is given by the expression

$$\int_0^{\infty} da' \int_{l-a' dt}^l da f(a, a') = dt \int_0^{\infty} da' a' f(l, a')$$

where $f(a, a')$ is the joint probability density function of the amplitude a and its time derivative $a' = da/dt$. The probability that a will cross the level l in the time interval t to $t+dt$ with a derivative of either sign is then

$$dt \int_{-\infty}^{\infty} |a'| f(l, a') da' .$$

For stationary processes, the mean number of level crossings of P in the interval t to $t+T$ then becomes

$$\langle N(P, T) \rangle = T \int_{-\infty}^{\infty} |a'| f(\sqrt{P}, a') da' .$$

The joint probability density function of the Rician distributed amplitude a and its time derivative a' is derived in Appendix B. This function is:

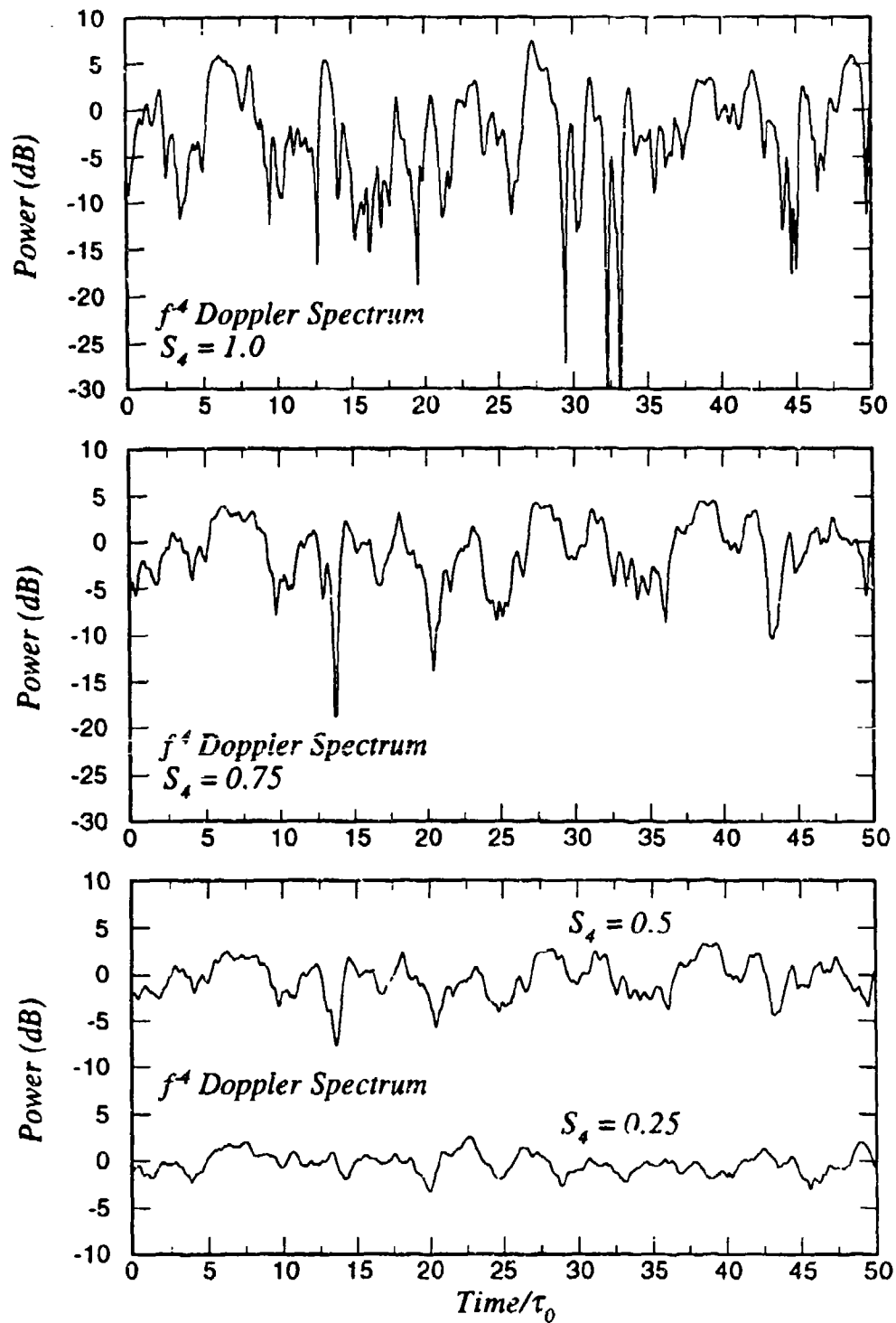


Figure 6. Realizations of Rician fading with f^{-4} Doppler spectra and scintillation indices of 1.0, 0.75, 0.5 and 0.25.

$$f(a, a') = \frac{2a}{P_0(1-R)} \exp\left[-\frac{a^2/P_0+R}{1-R}\right] I_0\left[\frac{2a\sqrt{R/P_0}}{1-R}\right] \\ \times \left[\frac{\tau_0}{\Delta\sqrt{2\pi P_0(1-R)}}\right] \exp\left[-\frac{(\tau_0 a')^2}{2\Delta^2 P_0(1-R)}\right] \\ (0 < a < \infty, -\infty < a' < \infty)$$

It can be seen from the form of this equation that the probability density function of a is Rician; the probability density function of a' is Gaussian with zero mean and variance of $\Delta^2 P_0(1-R)/\tau_0^2$; and a and a' are independent. Also the functional form of $f(a, a')$ is independent of the functional form of the Doppler spectrum. Only the parameter Δ varies with the Doppler spectrum ($\Delta = 1$ for the Gaussian spectrum, $\Delta = 1.1858$ for the f^{-6} spectrum, and $\Delta = 1.518$ for the f^{-4} spectrum).

The mean number of level crossings can now be easily evaluated with the result

$$\langle N(P, T) \rangle = \Delta \left(\frac{T}{\tau_0}\right) \left[\frac{8P/P_0}{\pi(1-R)}\right]^{\frac{1}{2}} \exp\left[-\frac{P/P_0+R}{1-R}\right] I_0\left[\frac{2\sqrt{RP/P_0}}{1-R}\right]$$

The effect of different Doppler spectra is to scale the mean number of level crossings by the quantity Δ . This fact was shown qualitatively by comparing the realizations with different spectra in Figure 5.

Figure 7 shows plots of the mean number of crossings of P in one decorrelation time versus the ratio P/P_0 for a Gaussian Doppler spectrum and several values of the scintillation index. For the Rayleigh case the maximum value of $\langle N(P, T) \rangle$ occurs at $P/P_0 = 1/2$ or -3 dB. As the scintillation index decreases the maximum value of $\langle N(P, T) \rangle$ approaches 0 dB.

By noting that two level crossings are required to define the beginning and end of a fade, the number of fades per unit time below the level P is $\eta = \langle N(P, \tau_0) \rangle / 2\tau_0$. The mean separation $\langle T_{sep}(P) \rangle$ of fades below P is then obtained from the mean number of fades per unit time. For any long time interval T the mean number of fades is ηT , and the mean separation is just $T/\eta T$ or $1/\eta$. Thus the mean separation of fades below P is

$$\langle T_{sep}(P) \rangle = \frac{2\tau_0}{\langle N(P, \tau_0) \rangle}$$

The mean separation of fades below P is equal to the average time between crossings of P with either a negative value of a' (which defines the start of the fade) or with positive value of a' (which defines the end of the fade). Thus the mean separation of fades below P is also equal to the mean separation of flares above P .

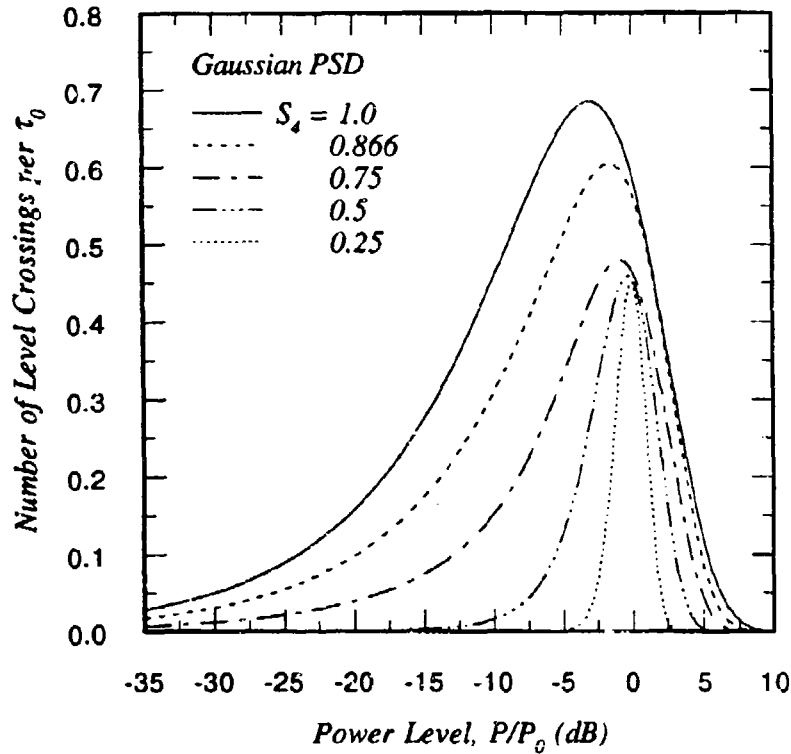


Figure 7. Mean number of level crossings per τ_0 for several scintillation indices.

The mean duration $\langle T_{Dur}(P) \rangle$ of fades below P is obtained as follows: During a long time interval T the total time that the power will be below P is $F(P)T$ where $F(P)$ is the cumulative distribution given in Equation 2.2. The mean duration is then the sum of all durations $F(P)T$ divided by the number of fades ηT . The result is

$$\langle T_{Dur}(P) \rangle = \frac{2\tau_0 F(P)}{\langle N(P, \tau_0) \rangle} .$$

The mean duration $\langle T_{Flare}(P) \rangle$ of a flare above P is the mean time that the power stays above P . Using the arguments given above, the mean separation of a fade or a flare is equal to the mean time that the signal is above P plus the mean time that it is below P , $\langle T_{Dur}(P) \rangle + \langle T_{Flare}(P) \rangle = \langle T_{Sep}(P) \rangle$. The mean duration of a flare is then

$$\langle T_{Flare}(P) \rangle = \frac{2\tau_0 [1-F(P)]}{\langle N(P, \tau_0) \rangle} .$$

The mean duration and separation of fades are shown in Figures 8 and 9, respectively, for a Gaussian Doppler spectrum and several values of the scintillation index. For other Doppler spectra, the curves in Figures 8 and 9 scale by $1/\Delta$.

The curves in Figure 8 show, for some power levels, that the duration of fades increases as the scintillation index is reduced. The mean duration of fades for S_4 equal to 0.75 exceeds that of Rayleigh fading at all power levels: the mean fade duration for S_4 equal to 0.5 exceeds that of Rayleigh fading except for P/P_0 values between -4 and -2 dB; and the mean fade duration for S_4 equal to 0.25 exceeds that of Rayleigh fading except for P/P_0 values between -13 and -1 dB. Note, however, that when S_4 is equal to 0.25 the probability of a 13 dB fade is 3.7×10^{-10} , and the mean separation of 13 dB fades is $7.4 \times 10^8 \tau_0$. Thus for S_4 values greater than about 0.25, it is possible to have fades that are longer than occur at the same level with full Rayleigh amplitude statistics.

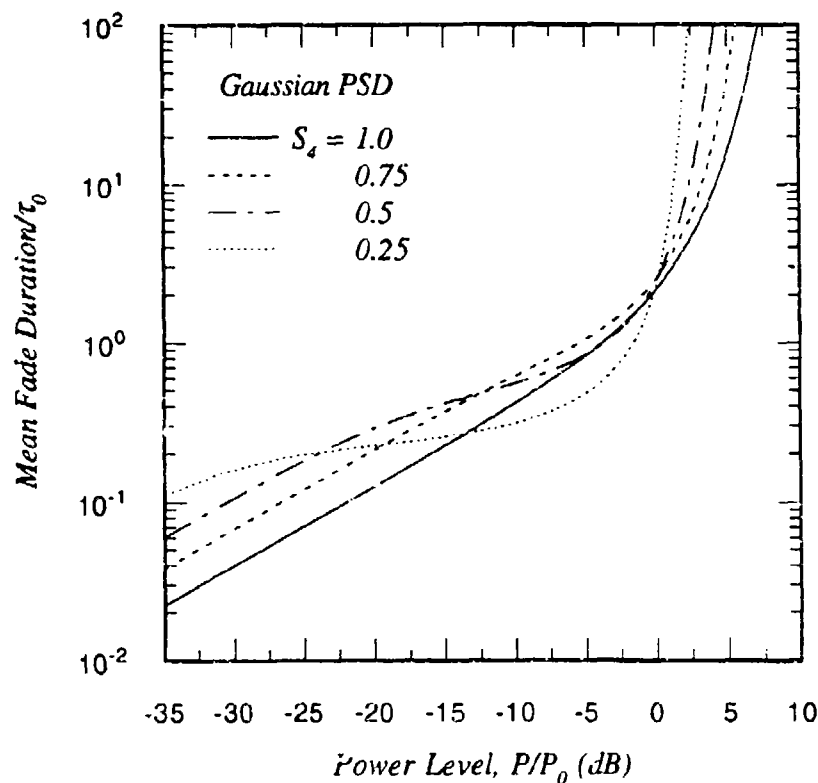


Figure 8. Mean duration of Rician distributed fades.

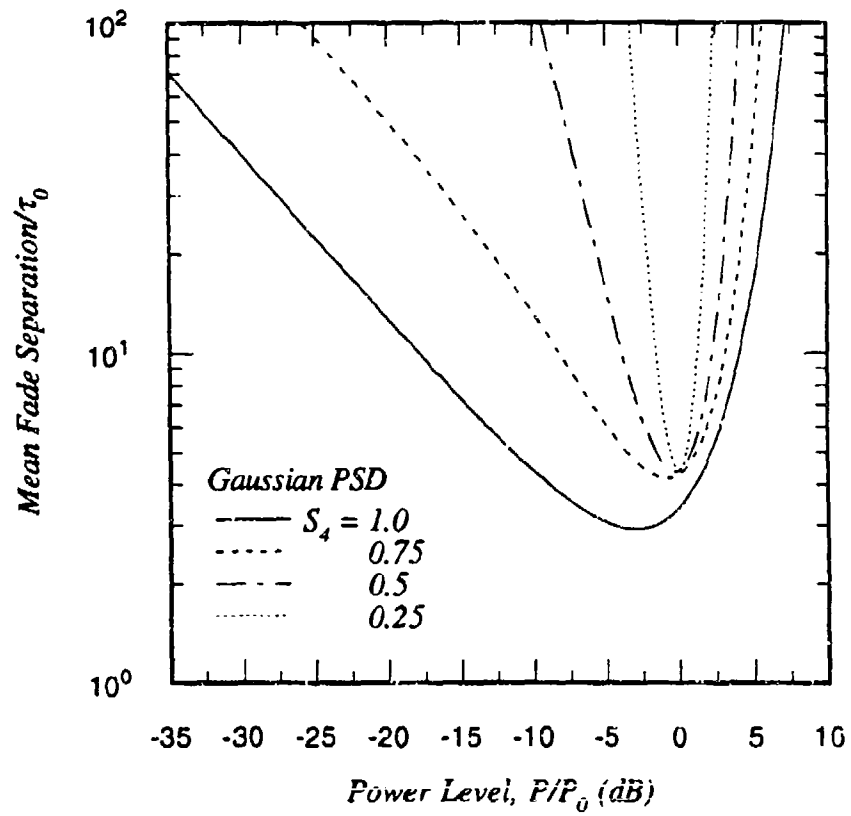


Figure 9. Mean separation of Rician distributed fades.

SECTION 3 SAMPLED Rician FADING

The requirements on the sampling of fading realizations are given in the DNA signal specification for nuclear scintillation [Wittwer, 1980] which requires a minimum of 100 decorrelation times per realization and 10 samples per decorrelation time. The questions that arise from this requirement can be summarized as: How close are such realizations to Rician fading? To address this question, random realizations of Rician fading are generated; moments of the amplitude, cumulative distribution, and mean fade duration and separation are measured; and these measured values are compared with their ensemble values.

Dana [1988] showed that $100\tau_0$ realizations of Rayleigh fading are adequate for fade depths of 20 dB or less, and that $400\tau_0$ realizations are necessary to simulate fades down to 30 dB. It was also shown in Dana [1988] that 10 samples per decorrelation time are sufficient when linear interpolation of the complex impulse response function is used to sample $h(k\Delta t_{Sam})$ 40 times per decorrelation time.

Thus results in this section are, for the most part, limited to $400\tau_0$ realizations sampled at $\Delta t_{Sam} = \tau_0/40$. Only the f^{-4} Doppler frequency PSD is considered for non-Rayleigh fading because this is the PSD recommended by DNA for slow, flat fading cases where the scintillation index is most likely to be less than unity.

Because of the finite number of samples in each realization, each measurement of realization statistics is a random variable with some mean and standard deviation. Variations in statistics from realization-to-realization are measured by generating a large number of realizations (1024 to be exact). Each parameter is measured by averaging over the entire realization. Average and standard deviation values of the 1024 measurements are computed. Thus the standard deviations below represent the realization-to-realization variation in the measurements of amplitude moments, cumulative distribution, and temporal statistics.

The measurement variation of the mean power of realizations can be calculated analytically, as discussed in Appendix C. It may be possible to compute measurement variances for other amplitude moments in the general case of Rician fading. Such a tedious exercise, however, is left to the determined reader. Power measurement variances below agree quite well with the analytic results given in Appendix C.

Three cases will be considered. The number of samples per realization N is 1024, 2048, or 4096, and the number of samples per decorrelation time N_0 is 10. Here N_0 is the number of samples per decorrelation time used to generate the realizations. Methods of generating such realizations are outlined in Appendix A. To measure the statistics of the realizations, linear interpolation of the real and imaginary parts of the impulse response function is used to obtain a sampling period Δt_{Sam} of $\tau_0/40$.

The objectives of this section are to present the means and standard deviations of amplitude moment, cumulative distribution, and temporal statistics, and to attempt to

answer the above question based on these results. This section is limited to flat fading realizations with varying values of the scintillation index and Doppler frequency power spectral density.

3.1 MEASURED FIRST ORDER STATISTICS.

One criterion for deciding that a realization has the proper Rician amplitude statistics is that measured moments of the amplitude should agree with Rician values within some tolerance. Ensemble values for the moments of the amplitude are obtained from Equation 2.1:

$$\langle a \rangle = \frac{1}{2} \left[\frac{\pi P_0}{1-R} \right]^{\frac{1}{2}} \exp \left[-\frac{R}{2(1-R)} \right] \left\{ I_0 \left[\frac{R}{2(1-R)} \right] + R I_1 \left[\frac{R}{2(1-R)} \right] \right\}$$

$$\langle a^2 \rangle = P_0$$

$$\langle a^3 \rangle = \frac{1}{4} \left[\frac{\pi P_0^3}{1-R} \right]^{\frac{1}{2}} \exp \left[-\frac{R}{2(1-R)} \right] \left\{ (3-R^2) I_0 \left[\frac{R}{2(1-R)} \right] + 2R(2-R) I_1 \left[\frac{R}{2(1-R)} \right] \right\}$$

$$\langle a^4 \rangle = P_0^2 (2-R^2)$$

where $I_0(\cdot)$ and $I_1(\cdot)$ are modified Bessel function.

These moments are plotted in Figure 10 versus the scintillation index for unity mean power. However, amplitude moments are easily obtained for other values of the mean power by noting that $\langle a^n \rangle$ scales as $P_0^{n/2}$.

The scintillation index S_4 is the standard deviation of the power. It is necessary but not sufficient that S_4 equal unity for Rayleigh fading. The scintillation index is a good measure of the statistics of flares but not of fades.

Statistics that are sensitive to the distribution of fades are moments of the log amplitude. Using Equation 2.1 and a little algebra, these moments are found to be:

$$\langle x \rangle = \langle \ln a \rangle = \frac{1}{2} \ln [P_0(1-R)] + \frac{1}{2} \exp \left[-\frac{R}{1-R} \right] \sum_{n=0}^{\infty} \left[\frac{R}{1-R} \right]^n \frac{\psi(n+1)}{\Gamma(n+1)}$$

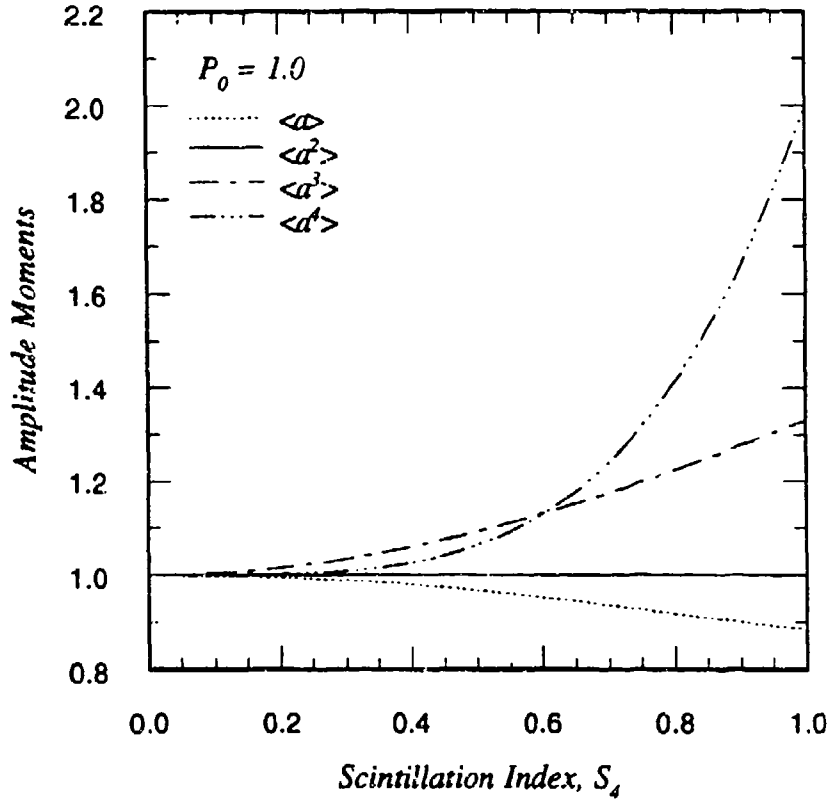


Figure 10. Amplitude moments of the Rician distribution.

$$\begin{aligned} \langle \chi^2 \rangle &= \langle \ln^2 a \rangle = \ln [P_0(1-R)] \langle \chi \rangle - \frac{1}{4} \ln^2 [P_0(1-R)] \\ &+ \frac{1}{4} \exp \left[-\frac{R}{1-R} \right] \sum_{n=0}^{\infty} \left[\frac{R}{1-R} \right]^n \frac{\psi^2(n+1) + \zeta(2, n+1)}{\Gamma(n+1)}. \end{aligned}$$

The ψ and ζ functions are:

$$\psi(n+1) = -\gamma + \sum_{k=1}^n \frac{1}{k} = \psi(n) + \frac{1}{n}$$

$$\zeta(2, n+1) = \sum_{k=n+1}^{\infty} \frac{1}{k^2} = \zeta(2, n) - \frac{1}{n^2}, \quad \zeta(2, 1) = \frac{\pi^2}{6}$$

where γ is Euler's constant ($\gamma = 0.5772157\dots$).

The first two moments of log amplitude are plotted in Figure 11 versus the scintillation index for unity mean power.

Measured values of the mean and standard deviation of the amplitude moments, S_4 , $\langle \chi \rangle$, and $\langle \chi^2 \rangle$ for Rician fading realizations are in Table 1 for eight cases including $100\tau_0$, $200\tau_0$, and $400\tau_0$ long realizations, three different Doppler frequency power spectral densities (PSDs), and four values of the scintillation index. Measured values for a single realization should equal the ensemble value plus or minus one or two standard deviations. It can be seen from the table that the average values are close to the ensemble values but the standard deviations of the higher amplitude moments can be as large as 20 percent of the measured values.

It is noteworthy that the measurement variation of $\langle \chi \rangle$ increases dramatically as the scintillation index is reduced while that of $\langle \chi^2 \rangle$ is relatively insensitive to S_4 . An explanation for this curious behavior has not been discovered.

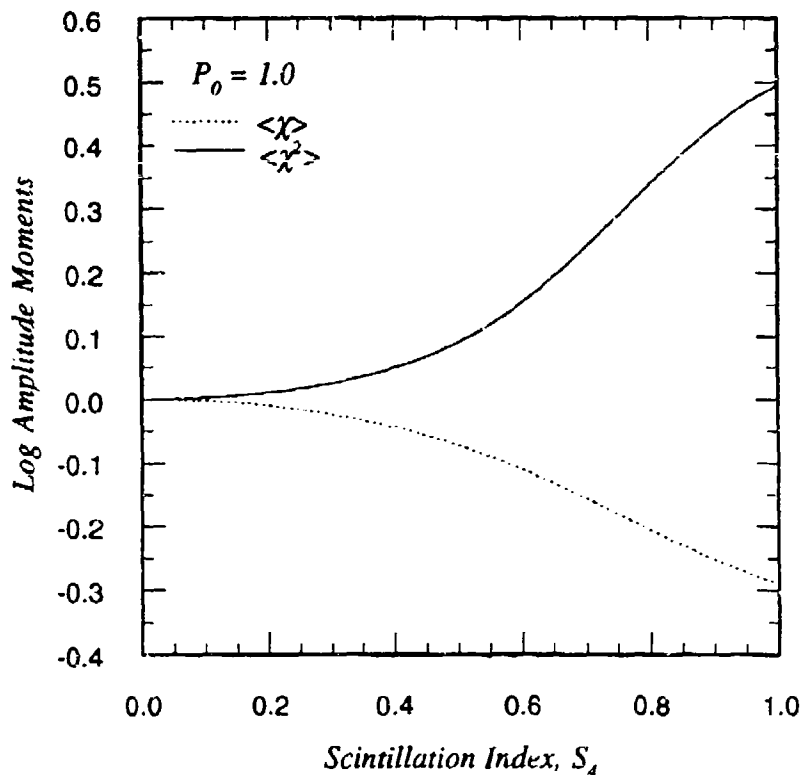


Figure 11. Log amplitude moments of the Rician distribution.

Table 1.
Statistics of sampled Rician fading realizations.

| | | Case | | | | | | | |
|---|----------|-------|--------|-------|----------|----------|----------|----------|----------|
| | | 1 | 2 | 3 | 4 | 5 | 6 | 7 | 8 |
| Ensemble Values | | | | | | | | | |
| N | | 1024 | 2048 | 4096 | 4096 | 4096 | 4096 | 4096 | 4096 |
| N_0 | | 10 | 10 | 10 | 10 | 10 | 10 | 10 | 10 |
| PSD | | Gauss | Gauss | Gauss | f^{-6} | f^{-4} | f^{-4} | f^{-4} | f^{-4} |
| S_4 | | 1.0 | 1.0 | 1.0 | 1.0 | 1.0 | 0.75 | 0.5 | 0.25 |
| Measured Values* (Normalized to Ensemble Values) | | | | | | | | | |
| $\langle a \rangle$ | μ | 0.999 | 0.998 | 0.999 | 0.997 | 0.996 | 0.998 | 0.999 | 1.000 |
| | σ | 0.054 | 0.040 | 0.029 | 0.028 | 0.027 | 0.027 | 0.018 | 0.009 |
| $\langle a^2 \rangle$ | μ | 0.998 | 0.996 | 0.998 | 0.994 | 0.991 | 0.996 | 0.998 | 0.999 |
| | σ | 0.105 | 0.077 | 0.056 | 0.054 | 0.053 | 0.049 | 0.034 | 0.017 |
| $\langle a^3 \rangle$ | μ | 0.995 | 0.993 | 0.997 | 0.991 | 0.988 | 0.994 | 0.997 | 0.999 |
| | σ | 0.161 | 0.0117 | 0.085 | 0.081 | 0.080 | 0.071 | 0.049 | 0.026 |
| $\langle a^4 \rangle$ | μ | 0.991 | 0.988 | 0.995 | 0.989 | 0.984 | 0.991 | 0.995 | 0.998 |
| | σ | 0.226 | 0.164 | 0.119 | 0.113 | 0.111 | 0.094 | 0.065 | 0.034 |
| S_4 | μ | 0.982 | 0.989 | 0.996 | 0.998 | 0.997 | 0.995 | 0.994 | 0.993 |
| | σ | 0.084 | 0.061 | 0.046 | 0.044 | 0.042 | 0.043 | 0.040 | 0.038 |
| $\langle \chi \rangle$ | μ | 1.000 | 1.005 | 1.004 | 1.013 | 1.017 | 1.004 | 1.003 | 1.009 |
| | σ | 0.213 | 0.155 | 0.114 | 0.109 | 0.106 | 0.180 | 0.273 | 0.548 |
| $\langle \chi^2 \rangle$ | μ | 0.996 | 1.000 | 1.001 | 1.007 | 1.009 | 0.993 | 0.991 | 0.990 |
| | σ | 0.153 | 0.111 | 0.081 | 0.075 | 0.072 | 0.121 | 0.124 | 0.085 |
| N_0 | μ | 1.018 | 1.011 | 1.004 | 0.998 | 0.999 | 0.999 | 0.999 | 0.999 |
| | σ | 0.083 | 0.056 | 0.038 | 0.048 | 0.055 | 0.055 | 0.055 | 0.054 |

* μ = Measured average value
 σ = Measured standard deviation

Perhaps a better criterion for the validity first order statistics is close agreement between the Rician and the measured cumulative distributions. Measured cumulative distributions (dots plus or minus one-sigma error bars) are plotted in Figures 12-16 for cases 5-8 in Table 1, respectively, along with the ensemble curves (Eqn. 2.2). A level of 0 dB corresponds to the mean power P_0 . It can be seen from the figures that $400\tau_0$ realizations do indeed have, on the average, a Rician distribution of fades.

3.2 MEASURED SECOND ORDER STATISTICS.

Table 1 also contains the mean and standard deviation of the measured number of samples per decorrelation time. The measured value of N_0 is obtained by performing an autocorrelation of the complex impulse response function and finding the e^{-1} point. Close agreement of this parameter with its ensemble value ensures that the realization will indeed have the desired decorrelation time in a simulation or hardware test.

The fidelity of the realizations in reproducing the second order statistics of Rician fading will be demonstrated by considering the mean fade duration and separation. The mean fade duration is a good statistic to examine for communications applications because errors often occur in bursts during deep fades. If the fades, on the average, are too long or too short, error bursts will not have the proper durations and the resulting receiver performance may be misleading.

Fade duration and separation measurements (dots plus or minus one-sigma error bars) and ensemble curves (solid lines) for the f^{-4} Doppler PSD are shown in Figures 16-19 for cases 5-8 respectively. Figure 16 shows these measurements for full Rayleigh fading. Good agreement between the measure and ensemble values is seen, except for 30 dB fades. At this level the ensemble fade duration is $0.026\tau_0$, which is quite close to the sample duration of $0.025\tau_0$. As the scintillation index is reduced, measured mean fade durations are generally close to, if not right on, the ensemble curves. However, large variations are seen in the measured mean fade separations.

Two effects contribute to the low mean fade separation measurements seen for scintillation indices less than unity. Because separation measurements require two fades, some realizations do not contribute to the realization-to-realization fade separation statistics, thereby reducing the measured average. Also, it is not possible in these realizations to measure fade separations larger than about $400\tau_0$. Thus measured mean separations are biased to lower values because large random samples are absent.

In Figure 19, for a scintillation index of 0.25, a large discrepancy in the measured mean fade duration and separation is seen at fade level of +3 dB. Here the mean fade duration is about $800\tau_0$, which clearly cannot be accurately measured in $400\tau_0$ realizations. Because the measured mean fade separation and measurement variance at this level are *not* zero, at least two realizations must have had two +3 dB flares even though the probability of such an event is less than 5×10^{-4} . The measured mean duration of 5 dB fades (which occur with a probability of approximately 3×10^{-4}) is close to the ensemble value of $0.31\tau_0$, but the measured mean fade separation is only ten percent of the ensemble value of $1042\tau_0$.

Except for low probability events with large durations or separations, these results demonstrate that $400\tau_0$ Rician fading realizations sampled at $\tau_0/40$ do indeed have the proper temporal statistics.

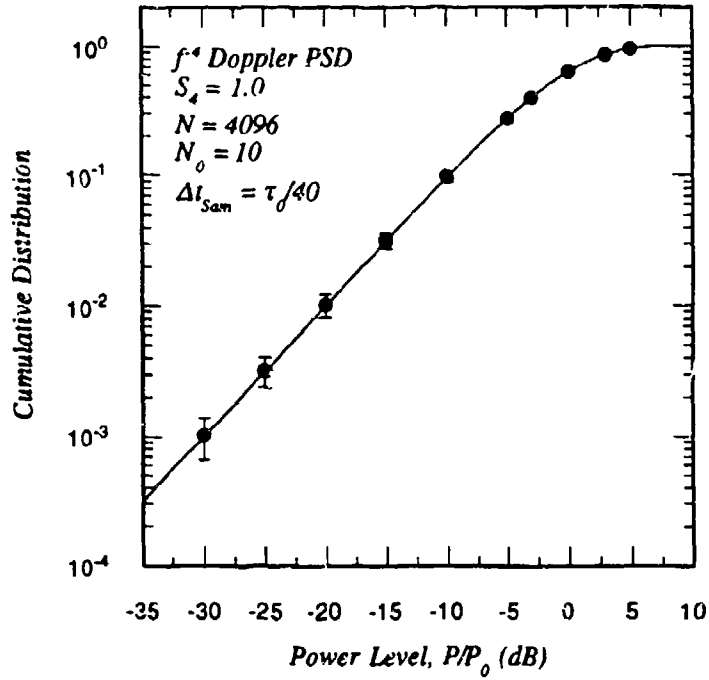


Figure 12. Measured cumulative distribution for $S_4 = 1.0$.

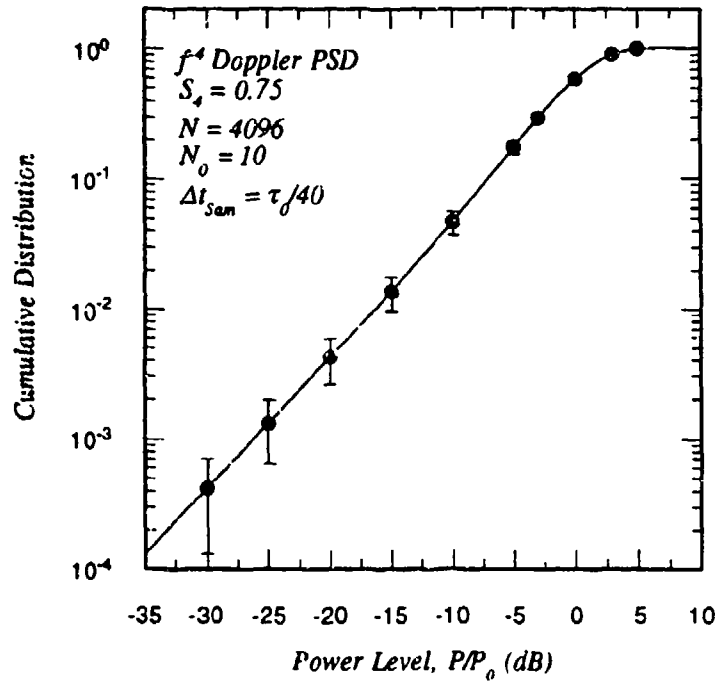


Figure 13. Measured cumulative distribution for $S_4 = 0.75$.

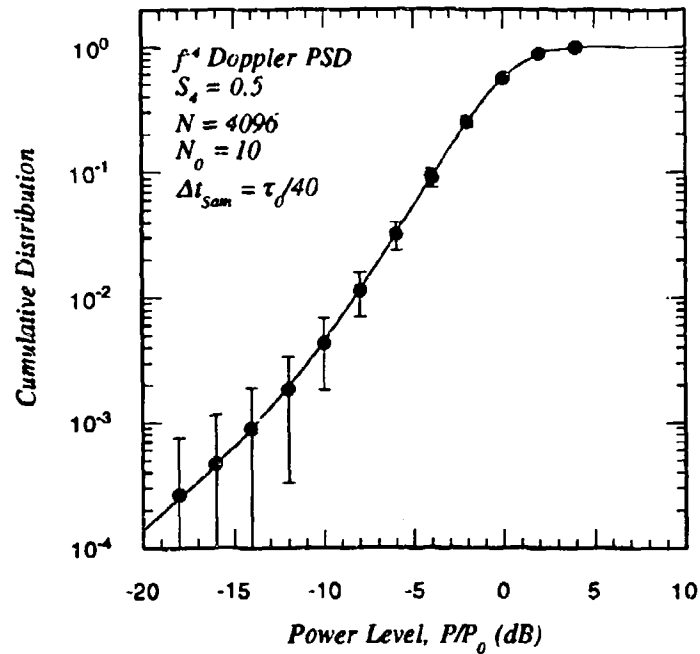


Figure 14. Measured cumulative distribution for $S_4 = 0.5$.

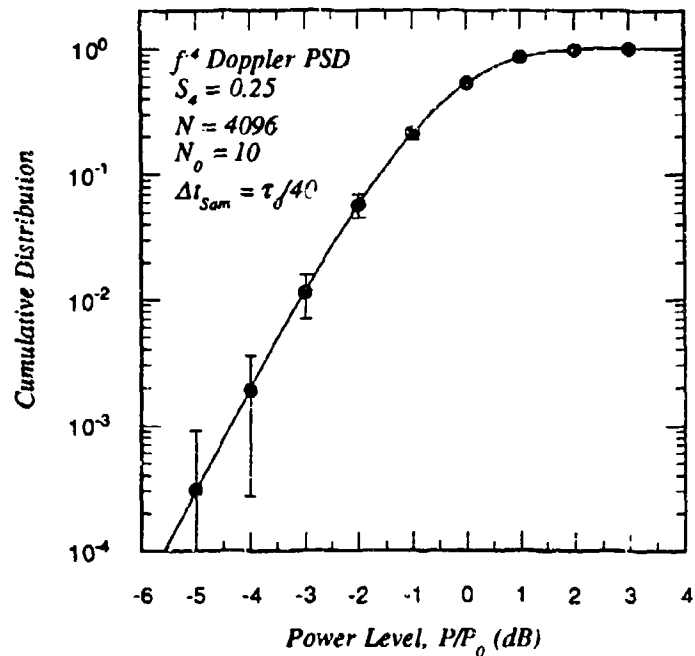


Figure 15. Measured cumulative distribution for $S_4 = 0.25$.

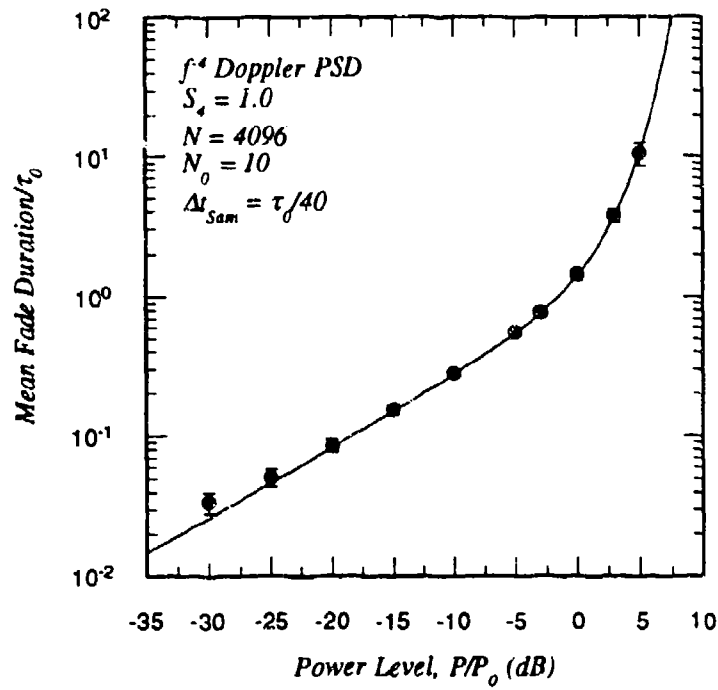


Figure 16a. Measured mean fade duration for $S_4 = 1.0$.

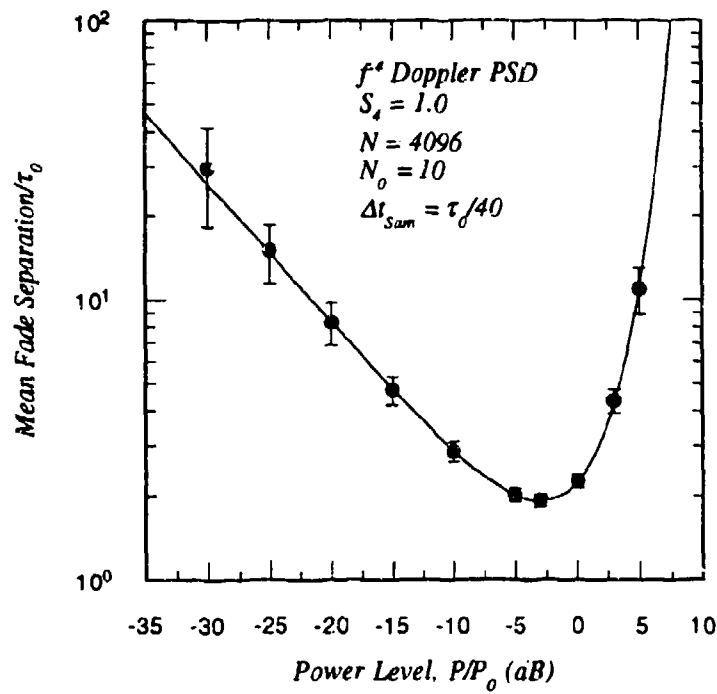


Figure 16b. Measured mean fade separation for $S_4 = 1.0$.

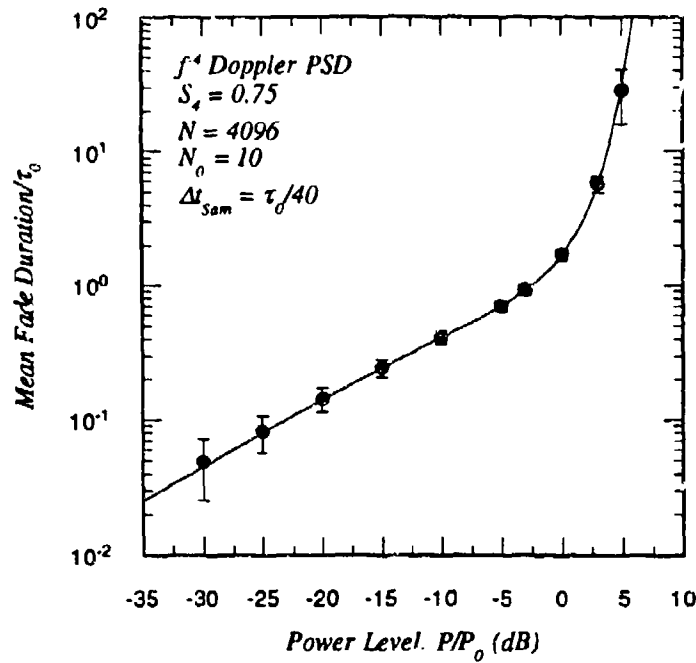


Figure 17a. Measured mean fade duration for $S_4 = 0.75$.

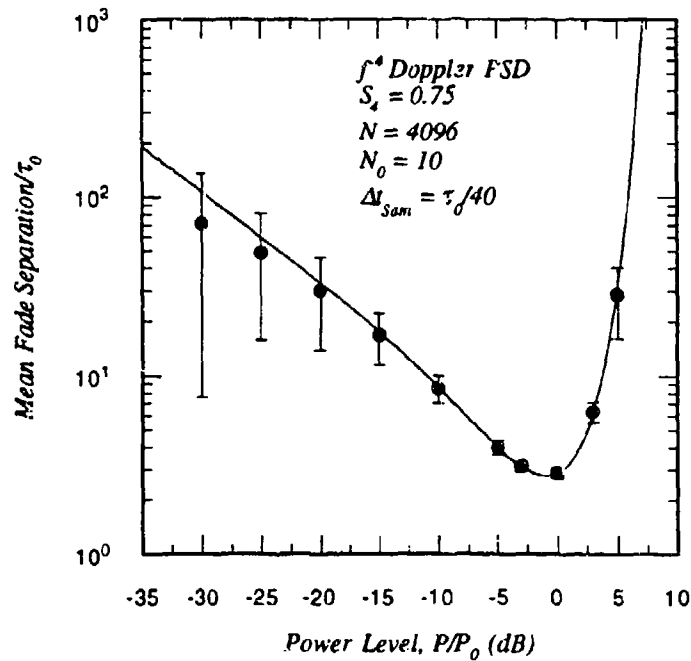


Figure 17b. Measured mean fade separation for $S_4 = 0.75$.

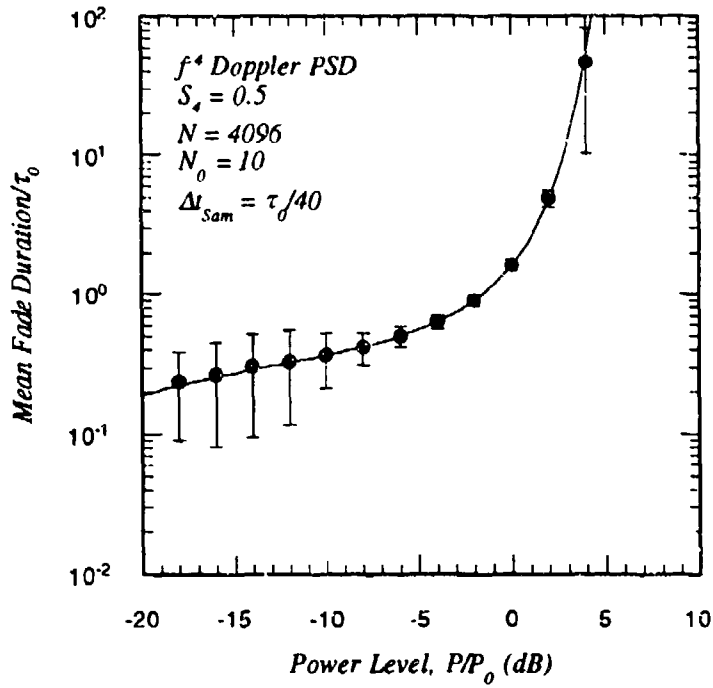


Figure 18a. Measured mean fade duration for $S_4 = 0.5$.

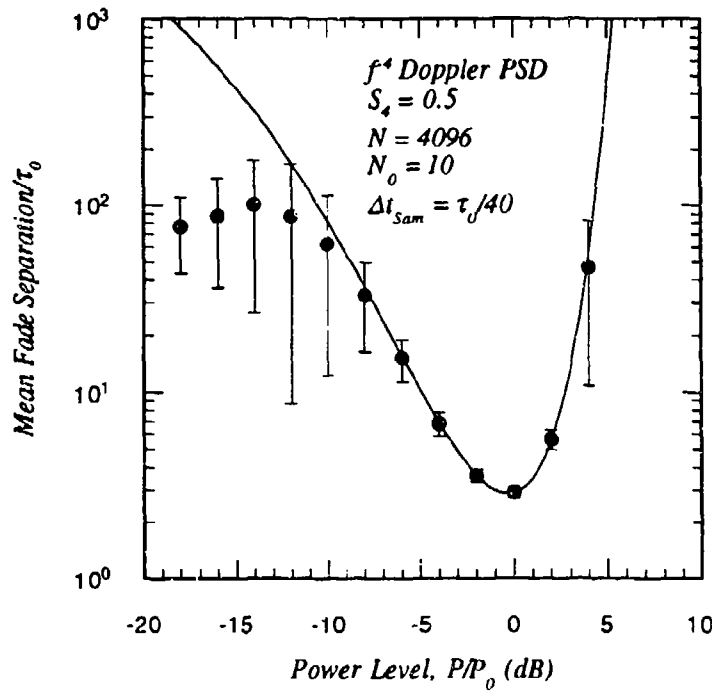


Figure 18b. Measured mean fade separation for $S_4 = 0.5$.

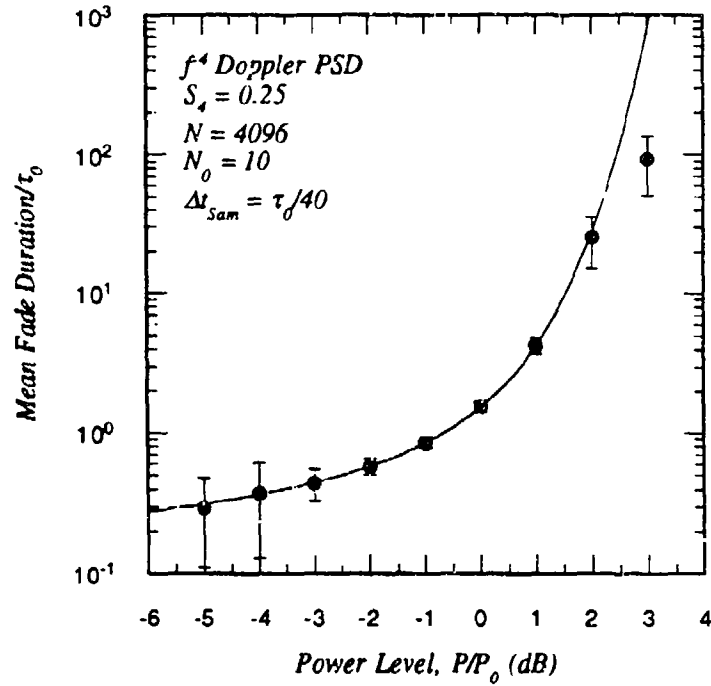


Figure 19a. Measured mean fade duration for $S_4 = 0.25$.

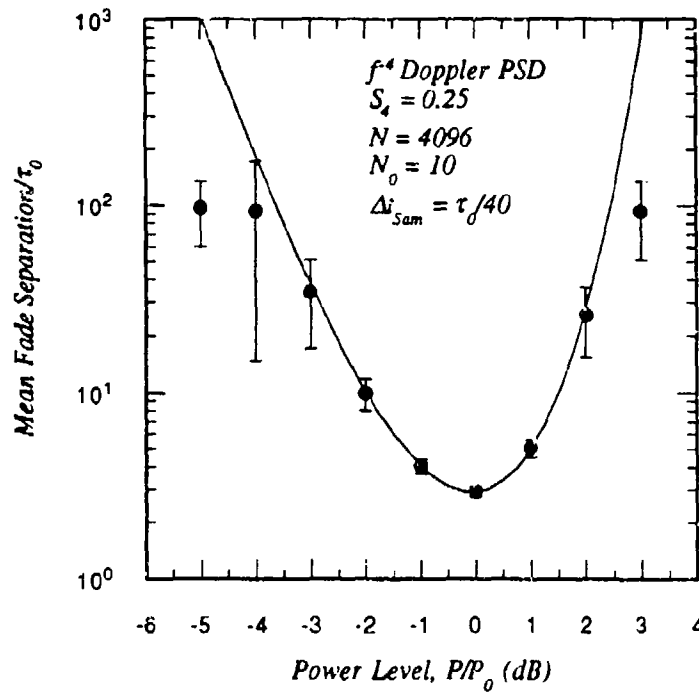


Figure 19b. Measured mean fade separation for $S_4 = 0.25$.

SECTION 4 LIST OF REFERENCES

- Bogusch, R. L., *Digital Communications in Fading Channels: Modulation and Coding*, AFWL-TR-87-52, MRC-R-1043, Mission Research Corporation, 1989.
- Dana, R. A., *Statistics of Sampled Rayleigh Fading*, DNA-TR-89-5, MRC-R-1203, Mission Research Corporation, April 1988.
- Dana, R. A., *ACIRF User's Guide for the General Model (Version 3.5)*, DNA-TR-91-162, MRC-R-1358, Mission Research Corporation, June 1991.
- Dana, R. A., *A Non-Stationary Model for Frequency Selective Channels*, MRC-R-1403, Mission Research Corporation, April 1992a.
- Dana, R. A., *Temporal Statistics of Non-Rayleigh Fading*, MRC-R-1429, Mission Research Corporation, December 1992b.
- De Raad, Jr., L. L., and M. K. Grover, *First-Order Intensity Statistics for Non-Rayleigh Fading*, DNA-TR-89-150, R&D Associates, February 1990.
- Frasier, S. M., *TEC Doppler and Delay Rate Realizations*, MRC-N-780, Mission Research Corporation, March 1988.
- Fremouw, E. J., R. C. Livingston, and D. A. Miller, "On the Statistics of Scintillating Signals," *J. Atmos. Terr. Phys.*, Vol. 42, pp. 717-731, 1980.
- Knepp, D. L., *Propagation of Wide Bandwidth Signals Through Strongly Turbulent Ionized Media*, DNA-TR-81-78, MRC-R-671, Mission Research Corporation, March 1982.
- Knepp, D. L., "Multiple Phase-Screen Calculation of the Temporal Behavior of Stochastic Waves," *Proc. IEEE*, Vol. 71, No. 6, pp. 722-737, June 1983.
- Knepp, D. L., and L. A. Wittwer, "Simulation of Wide Bandwidth Signals That Have Propagated Through Random Media," *Radio Science*, Vol. 19, No. 1, pp. 303-318, January-February 1984.
- Marcum, J. L., *A Statistical Theory of Target Detection by Pulsed Radar: Mathematical Appendix*, RM-753, RAND Corporation, July 1948.
- Rice, S. O., "Statistical Properties of a Sine Wave Plus Random Noise," *Bell System Technical Journal*, Vol. 27, pp. 109-157, January 1948.
- Rice, S. O., "Mathematical Analysis of Random Noise," in N. Wax (editor), *Selected Papers on Noise and Stochastic Processes*, Dover Publications, Inc., New York, 1954.
- Rice, S. O., "Distribution of the Duration of Fades in Radio Transmission: Gaussian Noise Model," *Bell System Technical Journal*, Vol. 37, pp. 581-635, May 1958.

Rino, C. L., and E. J. Fremouw, "Statistics for Ionospherically Diffracted VHF/UHF Signals," *Radio Science*, Vol. 8, No. 3, pp. 223-233, March 1973.

Rino, C. L., R. C. Livingston, and H. E. Whitney, "Some New Results on the Statistics of Radio Wave Scintillation, 1. Empirical Evidence for Gaussian Statistics," *J. Geophys. Res.*, Vol. 81, No. 13, pp. 2051-2057, 1976.

Whitney, H. E., J. Aarons, R. S. Allen, and D. R. Seeman, "Estimation of the Cumulative Amplitude Probability Distribution Function of Ionospheric Scintillations," *Radio Science*, Vol. 7, No. 12, pp. 1095-1104, December 1972.

Wittwer, L. A., *A Trans-Ionospheric Signal Specification for Satellite C³ Applications*, DNA 5662D, Defense Nuclear Agency, December 1980.

APPENDIX A REALIZATIONS OF RICIAN FADING

The methods of generating flat fading realizations of the impulse response function for Rician fading channels are simple extensions of Rayleigh fading methods discussed in detail elsewhere [e.g., *Knepp, 1982; Knepp and Wittwer, 1984; Dana, 1991; Dana 1992a*]. Only a brief review is presented this appendix.

The methods fall into two classes: Fourier transform and real-time digital filter techniques. The f^{-4} and f^{-6} Doppler Power Spectral Density (PSD) realizations are particularly simple to generate using digital filters. Realizations with a Gaussian Doppler PSD are more easily generated using Fourier transforms. These methods will be reviewed in subsections of this appendix.

A.1 FOURIER TRANSFORM TECHNIQUE FOR GAUSSIAN PSDs.

The starting point of the Fourier transform method of generating a realization of flat Rician fading is the Doppler frequency PSD function, $S(\omega_D)$. The Gaussian form of this function is:

$$S(\omega_D) = \sqrt{\pi} \tau_0 P_0 (1-R) \exp \left[-\frac{\tau_0^2 \omega_D^2}{4} \right] \quad (\text{Gaussian PSD})$$

where P_0 is the mean power of the realization, and $1-R$ is the fraction of power in the random component. The "Rician" index R is

$$R = \sqrt{1 - S_4^2}$$

where S_4 is the scintillation index. The quantity $S(\omega_D)d\omega_D/2\pi$ is the mean power in the Doppler radian frequency interval $\omega_D/2\pi$ to $(\omega_D + d\omega_D)/2\pi$.

Discrete realizations of the channel impulse response function will contain N time samples and N_0 samples per decorrelation time. Thus the time spacing of the discrete samples is

$$\Delta t = \frac{\tau_0}{N_0},$$

and the total time duration of the realization is $N\Delta t$. In the Doppler radian frequency domain the spacing of the discrete samples is

$$\Delta\omega_D = \frac{2\pi}{N\Delta t}.$$

Note that the quantity $\Delta\omega_D\Delta t$, which will appear later in a Fourier transform, is just $2\pi/N$.

The samples in the frequency domain are generated by first calculating the fraction of signal power in each Doppler frequency bin, $S_j = S(j\Delta\omega_D)\Delta\omega_D/2\pi$. For the Gaussian PSD,

$$S_j = \frac{\sqrt{\pi}P_0(1-R)N_0}{N} \exp\left[-\frac{j^2\pi^2N_0^2}{N^2}\right], \quad (j = -N/2, \dots, N/2-1) .$$

Next the random Doppler frequency spectrum $H(j\Delta\omega_D)$ of the impulse response function is generated:

$$H(j\Delta\omega_D) = \frac{2\pi}{\Delta\omega_D} \left[\sqrt{S_j} \xi_j + (\sqrt{P_0R} e^{i\varphi}) \delta_{j,0} \right] .$$

where R is the fraction of the total power in the constant component and φ is the constant phase of the Rician component. The quantity $\delta_{j,k}$ is the Kronecker delta symbol:

$$\delta_{j,k} = \begin{cases} 1 & j = k \\ 0 & \text{otherwise} \end{cases} .$$

The leading factor $2\pi/\Delta\omega_D$ has been included in $H(j\Delta\omega_D)$ so that the discrete Fourier transform of $H(j\Delta\omega_D)$ will be dimensionless. Random components of the spectrum, ξ_j , are complex, normally disturbed random variables with the properties:

$$\langle \xi_j \xi_k^* \rangle = \delta_{j,k}$$

$$\langle \xi_j \xi_k \rangle = 0 .$$

Thus the mean power of the ξ samples is unity. Random samples of ξ_j may be easily generated using

$$\xi_j = \sqrt{-\ln(u_{1j})} \exp(2\pi i u_{2j})$$

where u_{1j} and u_{2j} are independent random variables uniformly distributed on the interval [0,1).

Finally the random Doppler spectrum of the channel impulse response function is Fourier transformed to the time domain. In continuous notation this Fourier transform is

$$h(t) = \int_{-\infty}^{\infty} H(\omega_D) \exp(i\omega_D t) \frac{d\omega_D}{2\pi} ,$$

and in discrete notation,

$$\begin{aligned}
h(k\Delta t) &= \sum_{j=-N/2}^{N/2-1} H(j\Delta\omega_D) \exp [i(j\Delta\omega_D)(k\Delta t)] \frac{\Delta\omega_D}{2\pi} \\
&= \sum_{j=-N/2}^{N/2-1} \left[\sqrt{S_j} \xi_j + \left(\sqrt{P_0 R} e^{i\varphi} \right) \delta_{j,0} \right] \exp [2\pi i(jk/N)]
\end{aligned}$$

where $k = 0, 1, \dots, N-1$.

A.2 DIGITAL FILTER TECHNIQUE FOR f^{-4} AND f^{-6} PSDs.

An f^{-4} or f^{-6} realization can be generated by passing white Gaussian noise through cascaded single-pole filters, as described in Dana [1992a].

An f^{-4} filter can be created by cascading two single-pole filters:

$$\begin{aligned}
y_k &= ay_{k-1} + bx_{k-1} \\
x_k &= ax_{k-1} + bv_{k-1} .
\end{aligned} \tag{A.1}$$

The coefficients a and b are¹:

$$\begin{aligned}
a &= \exp(-\alpha_4 \Delta t / \tau_0) = \exp(-\alpha_4 / N_0) \\
b &= \sqrt{1-a^2}
\end{aligned}$$

where $\alpha_4 = 2.146193$. Discrete samples of the additive white Gaussian noise random process v_k are generated using the equation:

$$v_k = \left[\frac{(1-a^2)P_0(1-R)}{1+a^2} \right]^{\frac{1}{2}} \xi_k .$$

The v_k samples must have mean power given by the quantity in the square brackets so that the mean power of the filter output samples, y_k , will have mean power of $P_0(1-R)$. The discrete channel impulse response function in this case is

$$h(k\Delta t) = y_k + \sqrt{P_0 R} e^{i\varphi} .$$

To minimize the transient response at start-up it is necessary to initialize the filter. This is done by setting

¹ Some authors prefer to include the gain of the filter in b coefficients. For example, see Bogusch [1989] Equation 2-40. Wittwer [1980] writes the f^{-4} filter equations as shown here but he combines the exponential in the a coefficient with the expression for the mean power of the input white Gaussian noise to obtain a hyperbolic tangent function.

$$y_0 = \sqrt{P_0(1-R)} u_0$$

$$x_0 = \left[\frac{(1-a^2)P_0(1-R)}{1+a^2} \right]^{\frac{1}{2}} u_1 .$$

where u_0 and u_1 are independent samples of the random process ξ uncorrelated with the v_k samples. The y_1 and x_1 samples are obtained from Equation A.1 and the first v_k sample, v_0 . Even with this initialization there is a transient response because y_0 and x_0 do not have a "history" as they do after steady state is achieved. It is therefore suggested that the filter be "warmed up" for at least one decorrelation time before using the output.

An f^{-6} filter can be created by cascading three f^{-2} filters. The filter equations are therefore given by:

$$\begin{aligned} z_k &= az_{k-1} + by_{k-1} \\ y_k &= ay_{k-1} + bx_{k-1} \\ x_k &= ax_{k-1} + bv_{k-1} . \end{aligned} \tag{A.2}$$

The coefficients a and b are:

$$a = \exp(-\alpha_6 \Delta t / \tau_0) = \exp(-\alpha_6 / N_0)$$

$$b = \sqrt{1-a^2}$$

where $\alpha_6 = 2.904630$. Discrete samples of the additive white Gaussian noise random process v_k are generated using the equation:

$$v_k = \left[\frac{(1-a^2)^2 P_0(1-R)}{1+4a^2+a^4} \right]^{\frac{1}{2}} \xi_k .$$

Again the v_k samples must have mean power given by the quantity in the square brackets so that the mean power of the filter output samples, z_k , will have mean power of $P_0(1-R)$. The discrete channel impulse response function is

$$h(k\Delta t) = z_k + \sqrt{P_0 R} e^{i\varphi} .$$

Again, to minimize the transient response at start-up the initial filter values are:

$$z_0 = \sqrt{P_0(1-R)} u_0$$

$$y_0 = \left[\frac{(1-a^4)P_0(1-R)}{1+4a^2+a^4} \right]^{\frac{1}{2}} u_1$$

$$x_0 = \left[\frac{(1-a^2)^2 P_0(1-R)}{1+4a^2+a^4} \right]^{\frac{1}{2}} u_2$$

where u_0, u_1 , and u_2 are independent samples of complex AWGN uncorrelated with the v_k samples. The filter should be "warmed up" for at least one decorrelation time before the output is used.

A.3 WHAT ABOUT f^{-2} PSDs?

An obvious question is: Why not discuss generation of realizations with an f^{-2} Doppler PSD? Indeed the expressions for x_k in Equations A.1 and A.2 are single-pole filters that produce realizations with f^{-2} Doppler PSDs:

$$x_k = ax_{k-1} + bv_{k-1} .$$

For this simple case, the coefficients a and b are:

$$a = \exp(-\Delta t/\tau_0) = \exp(-1/N_0)$$

$$b = \sqrt{1-a^2} .$$

The problem with this Markov process is that the temporal statistics are, strictly speaking, undefined. This is because the scale factor Δ in the expression for the mean number of level crossings in Section 2.4 is

$$\Delta^2 = \frac{1}{2} \int_{-\infty}^{\infty} (\tau_0 \omega_D)^2 S(\omega_D) \frac{d\omega_D}{2\pi} . \quad (A.3)$$

For the f^{-2} Doppler PSD,

$$S(\omega_D) = \frac{2\tau_0}{1 + \tau_0^2 \omega_D^2} .$$

and the expression for Δ yields infinity.

Fortunately, for a discrete realization there is a maximum Doppler frequency determined by the sample spacing. The highest Doppler frequency component in the sampled realizations has a period $2\Delta t$, corresponding to a maximum frequency of:

$$\omega_{D,max} = \frac{\pi N_0}{\tau_0} .$$

The value of Δ for a sampled realization is then:

$$\Delta^2 = N_0 - \frac{\tan^{-1}(\pi N_0)}{\pi} .$$

For integer values of N_0 this expression reduces to N_0 .

Thus the mean number of level crossing is finite and the mean duration and separation of fades are non-zero. Unfortunately these quantities depend on N_0 . As the number of samples per decorrelation time is increased, the mean number of level crossing increases and the mean fade duration decreases.

The dependence of the temporal statistics of the f^{-2} Doppler PSD realization on N_0 is likely to be unacceptable in most applications. Thus only Doppler PSDs with a frequency roll-off greater than f^{-3} (so Eqn. A.3 is finite) should be used to generate realizations of Rician fading. This will ensure that the realization temporal statistics are well-behaved.

APPENDIX B

JOINT PROBABILITY DENSITY FUNCTION $f(a, a')$

The purpose of this appendix is to derive the joint probability density function of the Rician amplitude a and its time derivative $a' = da/dt$. This function is required to calculate the temporal statistics of Rician fading. A less general form of this derivation was first published by Rice [1948].

The starting point for this calculation is the determination of the joint probability density function of the random in-phase and quadrature components x and y of the complex envelope of the electric field. It is assumed that x and y are independent, have zero mean, and that they are normally distributed. Thus the joint probability density function of x and y is

$$f(x, y) = \frac{1}{2\pi\sigma^2} \exp\left[-\frac{x^2 + y^2}{2\sigma^2}\right]. \quad (\text{B.1})$$

Now the joint probability density function of the time derivatives $x' = dx/dt$ and $y' = dy/dt$ must be calculated. It will be shown that x and x' are independent, as are y and y' . It will be assumed that x , x' , y , and y' are jointly independent. Thus the joint probability density function of x' and y' is all that is needed in addition to Equation B.1 to write down the joint probability density function $f(x, x', y, y')$. Once this function has been obtained, a simple change of variables from x , x' , y , and y' to a and a' will yield the desired function.

In order to determine the distribution of x' (or y'), consider the random function $x(t)$ written as a Fourier stochastic integral

$$x(t) = \int_{-\infty}^{\infty} z(\omega_D) \exp(i\omega_D t) \frac{d\omega_D}{2\pi}. \quad (\text{B.2})$$

The quantity $z(\omega_D)$ is a random function in the Doppler frequency domain. It is useful to assume that $z(\omega_D)$ is a zero-mean, normally distributed random process, although this is not necessary because the central limit theorem will make $x(t)$ normally distributed for almost any reasonable distribution of $z(\omega_D)$. However, with the normal assumption for $z(\omega_D)$, $x(t)$ is the sum of many independent, normally distributed random variables, and is necessarily a zero-mean, normally distributed random variable.

Before continuing, it is interesting to show the relationship between the random spectral components $z(\omega_D)$ and the Doppler spectrum $S(\omega_D)$. The correlation function of the stationary process $x(t)$ may be written as

$$\begin{aligned} \rho(t_2-t_1) &= \frac{\langle x(t_1)x(t_2) \rangle}{\sigma^2} & (B.3) \\ &= \int_{-\infty}^{\infty} \frac{d\omega_{D1}}{2\pi} \int_{-\infty}^{\infty} \frac{d\omega_{D2}}{2\pi} \frac{\langle z(\omega_{D1})z^*(\omega_{D2}) \rangle}{\sigma^2} \exp(i\omega_{D1}t_1 - i\omega_{D2}t_2) . \end{aligned}$$

However the correlation function $\rho(\tau)$ may also be written in terms of $S(\omega_D)$:

$$\rho(\tau) = \int_{-\infty}^{\infty} S(\omega_D) \exp(i\omega_D\tau) \frac{d\omega_D}{2\pi} . \quad (B.4)$$

The spectrum $S(\omega_D)$ must be an even function if the correlation function $\rho(\tau)$ is to be real.

To ensure the integral in Equation B.3 is only a function of time difference $\tau=t_1-t_2$, the integrand must contain a factor $2\pi\delta(\omega_{D1}-\omega_{D2})$. Using the Dirac delta function to collapse the double integral in Equation B.3 and comparing the result with Equation B.4 gives

$$\langle z(\omega_{D1})z^*(\omega_{D2}) \rangle = 2\pi\sigma^2 \delta(\omega_{D1}-\omega_{D2}) S(\omega_{D1}) . \quad (B.5)$$

This equation also demonstrates that the random Doppler spectral components of $z(\omega_D)$ are uncorrelated, which is a consequence of the assumption that the random process $x(t)$ is stationary.

The time derivative of $x(t)$ is given by differentiating Equation B.2, with a similar expression holding for y' :

$$x'(t) = \int_{-\infty}^{\infty} (i\omega_D) z(\omega_D) \exp(i\omega_D t) \frac{d\omega_D}{2\pi} .$$

Because $z(\omega_D)$ is normally distributed with zero mean, $x'(t)$ will also be normally distributed with zero mean. The variance of $x'(t)$ is

$$\begin{aligned} \langle x'(t)x'(t) \rangle &= \int_{-\infty}^{\infty} \frac{d\omega_{D1}}{2\pi} \int_{-\infty}^{\infty} \frac{d\omega_{D2}}{2\pi} \omega_{D1}\omega_{D2} \langle z(\omega_{D1})z^*(\omega_{D2}) \rangle \exp [i(\omega_{D1}-\omega_{D2})t] \\ &= \sigma^2 \int_{-\infty}^{\infty} \omega_D^2 S(\omega_D) \frac{d\omega_D}{2\pi} = -\sigma^2 \left. \frac{d^2\rho(\tau)}{d\tau^2} \right|_{\tau=0} . \end{aligned} \quad (B.6)$$

The variance of $x'(t)$ may be written in the general form:

$$\langle x'(t)x'(t) \rangle = \frac{2\sigma^2\Delta^2}{\tau_0^2}$$

where

$$\Delta = \begin{cases} 1 & \text{Gaussian Doppler PSD} \\ \alpha_6/\sqrt{6} = 1.1858 & f^{-6} \text{ Doppler PSD} \\ \alpha_4/\sqrt{2} = 1.5176 & f^{-4} \text{ Doppler PSD} \end{cases}$$

and where the parameters α_4 and α_6 were determined in Section 2.2.

The cross correlation of $x'(t)$ and $x(t)$ is

$$\begin{aligned} \langle x'(t)x(t) \rangle &= \int_{-\infty}^{\infty} \frac{d\omega_{D1}}{2\pi} (i\omega_{D1}) \int_{-\infty}^{\infty} \frac{d\omega_{D2}}{2\pi} \langle z(\omega_{D1})z^*(\omega_{D2}) \rangle \exp [i(\omega_{D1}-\omega_{D2})t] \\ &= -i\sigma^2 \int_{-\infty}^{\infty} \omega_D S(\omega_D) \frac{d\omega_D}{2\pi} = 0 . \end{aligned} \quad (\text{B.7})$$

Equation B.5 and the fact that $S(\omega_D)$ is an even function have been used in reducing Equations B.6 and B.7. Because $x(t)$ and $x'(t)$ are uncorrelated and normally distributed, they are also independent. Identical results hold for the variance of y' and the cross correlation of y and y' .

The joint probability density function of $x, x', y,$ and y' may now be written down:

$$f(x,x',y,y') = \left(\frac{1}{2\pi\sigma^2} \right) \exp \left[-\frac{x^2+y^2}{2\sigma^2} \right] \left(\frac{\tau_0^2}{4\pi\sigma^2\Delta^2} \right) \exp \left[-\frac{\tau_0^2(x'^2+y'^2)}{4\sigma^2\Delta^2} \right] .$$

This function may be transform to the desired function of a and a' by making the change of variables

$$x + r \cos \vartheta = a \cos \theta$$

$$y + r \sin \vartheta = a \sin \theta$$

where r is the constant component of Rician fading and ϑ is the constant phase. The time derivatives of x and y are

$$x' = a' \cos \theta - a\theta \sin \theta$$

$$y' = a' \sin \theta + a\theta \cos \theta$$

which gives the polar coordinate equations

$$x^2 + y^2 = a^2 + r^2 - 2ar \cos(\theta - \vartheta)$$

$$x'^2 + y'^2 = a'^2 + a^2\theta^2$$

The probability density function coordinate transformation is

$$f(x, x', y, y') dx dx' dy dy' = f(a, a', \theta, \theta') | \det(J) | da da' d\theta d\theta'$$

where the determinate of the Jacobian of the transformation is

$$\begin{aligned} \det(J) &= \det \begin{bmatrix} \frac{\partial x}{\partial a} & \frac{\partial x'}{\partial a} & \frac{\partial y}{\partial a} & \frac{\partial y'}{\partial a} \\ \frac{\partial x}{\partial a'} & \frac{\partial x'}{\partial a'} & \frac{\partial y}{\partial a'} & \frac{\partial y'}{\partial a'} \\ \frac{\partial x}{\partial \theta} & \frac{\partial x'}{\partial \theta} & \frac{\partial y}{\partial \theta} & \frac{\partial y'}{\partial \theta} \\ \frac{\partial x}{\partial \theta'} & \frac{\partial x'}{\partial \theta'} & \frac{\partial y}{\partial \theta'} & \frac{\partial y'}{\partial \theta'} \end{bmatrix} \\ &= \det \begin{bmatrix} \cos \theta & -\theta' \sin \theta & \sin \theta & \theta' \cos \theta \\ 0 & \cos \theta & 0 & \sin \theta \\ -a \sin \theta & -a' \sin \theta - a\theta' \cos \theta & a \cos \theta & a' \cos \theta - a\theta' \sin \theta \\ 0 & -a \sin \theta & 0 & a \cos \theta \end{bmatrix} \\ &= a^2 \end{aligned}$$

The joint probability density function $f(a, a', \theta, \theta')$ is

$$\begin{aligned} f(a, a', \theta, \theta') &= \left(\frac{a^2}{2\pi\sigma^2} \right) \exp \left[-\frac{a^2 + r^2 - 2ar \cos(\theta - \vartheta)}{2\sigma^2} \right] \\ &\quad \times \left(\frac{\tau_0^2}{4\pi^2 \Delta^2 \sigma^2} \right) \exp \left[-\frac{\tau_0^2 (a'^2 + a\theta'^2)}{4\Delta^2 \sigma^2} \right] \end{aligned}$$

The joint probability density function of a and a' is obtained by integrating this equation over θ and θ' :

$$f(a, a') = \int_0^{2\pi} d\theta \int_{-\infty}^{\infty} d\theta' f(a, a', \theta, \theta') ,$$

with the result

$$f(a, a') = \left(\frac{a}{\sigma^2} \right) \exp \left[-\frac{a^2 + r^2}{2\sigma^2} \right] I_0 \left[\frac{ar}{\sigma^2} \right] \left(\frac{\tau_0}{2\sqrt{\pi}\Delta\sigma} \right) \exp \left[-\frac{\tau_0^2 a'^2}{4\Delta^2\sigma^2} \right] . \quad (\text{B.8})$$

I_0 is the modified Bessel function that results from performing the integral:

$$I_0(z) = \frac{1}{2\pi} \int_0^{2\pi} \exp(z \cos \theta) d\theta .$$

Thus it is apparent from Equation B.8 that the probability density function of a is Rician; the probability density function of a' is normal with zero mean and variance of $2\Delta^2\sigma^2/\tau_0^2$; and a and a' are independent because their joint probability density function is separable into a function of a times a function of a' .

APPENDIX C VARIATION IN THE MEASUREMENT OF MEAN POWER

The n^{th} moment of the amplitude a_k of an impulse response function realization with N samples is measured using the formula

$$\mu_n = \frac{1}{N} \sum_{k=1}^N a_k^n .$$

Because of the finite length of a realization, μ_n is a random variable. The purpose of this appendix is to develop general expressions for the mean and variance of μ_n , and then to apply those expressions to compute the expected variation, σ_μ^2 , in the measured mean power of a realization:

$$\sigma_\mu^2 = \langle \mu_n^2 \rangle - \langle \mu_n \rangle^2 .$$

This variation depends primarily on the number of decorrelation times in the realization, N/N_0 , where N_0 is the number of samples per decorrelation time. It is weakly dependent on the Doppler frequency power spectral density (PSD) and on the values of N and N_0 .

The mean value of μ_n is easy to compute:

$$\langle \mu_n \rangle = \frac{1}{N} \sum_{k=1}^N \langle a_k^n \rangle = \langle a^n \rangle$$

where $\langle a^n \rangle$ is the ensemble mean value of the n^{th} moment of amplitude. The second moment of μ_n is a little more of a challenge to compute:

$$\langle \mu_n^2 \rangle = \frac{1}{N^2} \sum_{k=1}^N \sum_{l=1}^N \langle a_k^n a_l^n \rangle = \frac{\langle a^{2n} \rangle}{N} + \frac{2}{N} \sum_{k=1}^{N-1} (1-k/N) R_n(k)$$

where $R_n(k)$ is the correlation of the n^{th} moment of amplitude:

$$R_n(k) = \langle a_l^n a_{l+k}^n \rangle .$$

For the general case of Rician fading and arbitrary n , the joint probability density function of the amplitude at two times, $f(a_1, a_2)$, is needed to compute the correlation function. However in the special case of mean power where n is two, the correlation function is easily computed from the statistics of the underlying complex voltage.

The power in a sample of the impulse response function with a Rician amplitude distribution is

$$a_k^2 = [x_k + r \cos \vartheta]^2 + [y_k + r \sin \vartheta]^2 \quad (\text{C.1})$$

where x_k and y_k are uncorrelated, normally-distributed random processes with zero-mean and variance σ^2 . The "Rician" components $r \cos \vartheta$ and $r \sin \vartheta$ are constant. It is assumed that the random processes x at two times is jointly normal:

$$f(x_1, x_2) = \frac{1}{2\pi\sigma^2\sqrt{1-\rho^2}} \exp\left[-\frac{x_1^2 - 2\rho x_1 x_2 + x_2^2}{2\sigma^2(1-\rho^2)}\right].$$

Values of the two-point correlation ρ are determined by the functional form of the Doppler PSD and the time difference between the samples x_1 and x_2 . A similar expression holds for the joint probability density function of y_1 and y_2 .

To compute the variance of the mean power measurement, the quantity $\langle a_1^2 a_2^2 \rangle$ is required. Using Equation C.1 this quantity involves terms of the form

$$\begin{aligned}\langle x_1 \rangle &= \langle x_2 \rangle = \langle y_1 \rangle = \langle y_2 \rangle = 0 \\ \langle x_1^2 \rangle &= \langle x_2^2 \rangle = \langle y_1^2 \rangle = \langle y_2^2 \rangle = \sigma^2 \\ \langle x_1 x_2 \rangle &= \langle y_1 y_2 \rangle = \sigma^2 \rho \\ \langle x_1 x_2^2 \rangle &= \langle x_1^2 x_2 \rangle = \langle y_1 y_2^2 \rangle = \langle y_1^2 y_2 \rangle = 0 \\ \langle x_1^2 x_2^2 \rangle &= \langle y_1^2 y_2^2 \rangle = \sigma^4(1 + 2\rho^2).\end{aligned}$$

The cross correlation $\langle a_1^2 a_2^2 \rangle$ is then

$$\langle a_1^2 a_2^2 \rangle = 4\sigma^4(1 + \rho^2) + 4r^2\sigma^2(1 + \rho) + r^4.$$

The Rician amplitude r and the variance σ^2 are written in terms of the scintillation index S_4 so that the mean power $\langle a^2 \rangle$ is constant and equal to P_0 :

$$\begin{aligned}r^2 &= P_0 R \\ 2\sigma^2 &= P_0(1-R)\end{aligned}$$

where the "Rician" index is

$$R = \sqrt{1 - S_4^2}.$$

Combining these results gives the following expression for the variance in the measured mean power:

$$\frac{\sigma_{\bar{P}}^2}{P_0^2} = \frac{1 - NR^2}{N} + \frac{2}{N} \sum_{k=1}^{N-1} (1 - k/N) [R + (1-R)\rho(k)]^2. \quad (C.2)$$

The two-point correlation $\rho(k)$ is

$$\rho(k) = \begin{cases} \exp [-(k/N_0)^2] & \text{Gaussian Doppler PSD} \\ [1 + \alpha_6 k/N_0 + (\alpha_6 k/N_0)^2/3] \exp [-\alpha_6 k/N_0] & f^{-6} \text{ Doppler PSD} \\ [1 + \alpha_4 k/N_0] \exp [-\alpha_4 k/N_0] & f^{-4} \text{ Doppler PSD} \end{cases}$$

where the coefficients α_4 ($\alpha_4=2.146139$) and α_6 ($\alpha_6=2.904630$) are determined by the requirement that $\rho(N_0)=e^{-1}$.

Plots of the power measurement standard deviation are shown in Figure 20 for N equal to 1024, 2048, and 4096. The value of N_0 is 10 for each case, so the curves correspond to realizations of length $102.4\tau_0$, $204.8\tau_0$, and $409.6\tau_0$, respectively. Solid lines in the figure are for a Gaussian Doppler frequency PSD, and solid circles are for an f^{-4} Doppler PSD.

As expected, the mean power measurement variation is larger for realizations with fewer decorrelation times. The measurement variation decreases with decreasing scintillation index because the fluctuating part of the impulse response contributes less and less to the total power. For a given value of N there is little difference between the results for the two PSDs. This is because the three correlation functions above differ little for values of k less than N_0 where $\rho(k)$ is close to unity, but vary significantly for larger values of k where $\rho(k)$ is small. Thus the differences in $\rho(k)$ for differing Doppler frequency PSDs occur in Equation C.2 at values of k that contribute little to the sum.

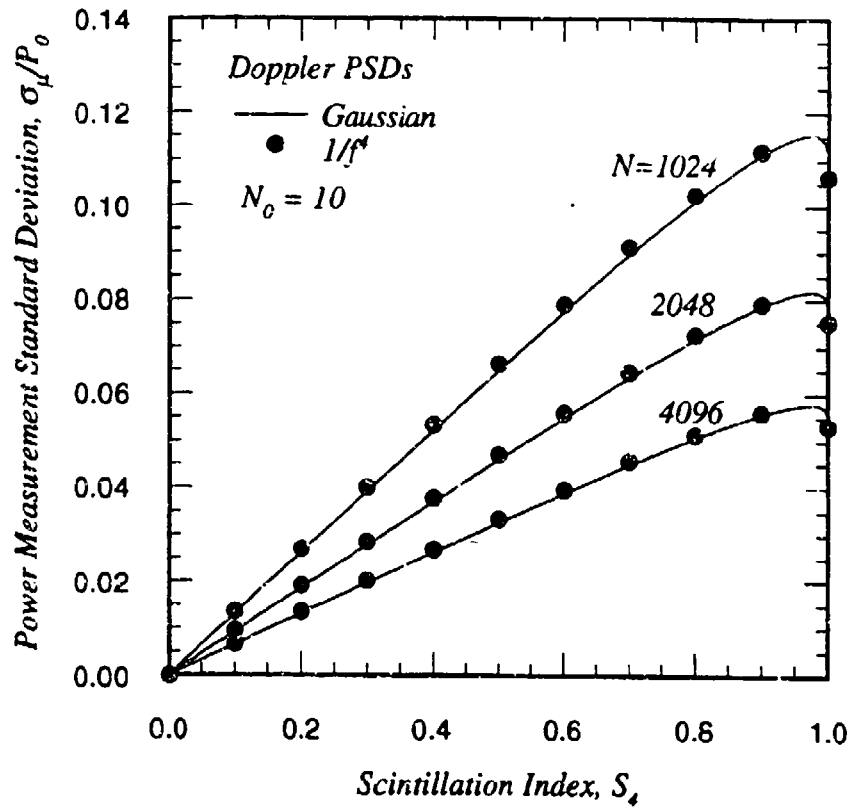


Figure 20. Power measurement error.

DISTRIBUTION LIST

DNA-TR-92-98

DEPARTMENT OF DEFENSE

ASSISTANT TO THE SECRETARY OF DEFENSE
ATTN: EXECUTIVE ASSISTANT

DEFENSE ADVANCED RSCH PROJ AGENCY
ATTN: CHIEF SCIENTIST
ATTN: GSD R ALEWINE

DEFENSE COMMUNICATIONS ENGINEER CENTER
ATTN: CODE R430 BOEHM

DEFENSE INFORMATION SYSTEMS
ATTN: SSS

DEFENSE INTELLIGENCE AGENCY
ATTN: DB-TPO
ATTN: DC-6
ATTN: DIR
ATTN: DIW-4
ATTN: DT-1B

DEFENSE NUCLEAR AGENCY
ATTN: NANF
ATTN: NASF
ATTN: OPNA
ATTN: RAAE
ATTN: RAAE CAPT J MEYERS
ATTN: RAAE CAPT T BAZZOLI
3 CYS ATTN: RAAE K SCHWARTZ
ATTN: RAAE R COX
ATTN: RAAE R JONES
ATTN: RAAE
ATTN: SPSD
2 CYS ATTN: TITL

DEFENSE TECHNICAL INFORMATION CENTER
2 CYS ATTN: DTIC/FDAB

FIELD COMMAND DEFENSE NUCLEAR AGENCY
ATTN: FCNM
ATTN: FCPRA LTC R HEDTKE

JOINT DATA SYSTEM SUPPORT CTR
ATTN: JNSV

STRATEGIC AND THEATER NUCLEAR FORCES
ATTN: DR E SEVIN
ATTN: DR SCHNEITER

STRATEGIC DEFENSE INITIATIVE ORGANIZATION
ATTN: EN
ATTN: EN LTC C JOHNSON
ATTN: TDW
ATTN: TNS

U S NUCLEAR CMD & CENTRAL SYS SUP STAFF
ATTN: SAB H SEQUINE

DEPARTMENT OF THE ARMY

ARMY LOGISTICS MANAGEMENT CTR
ATTN: DLSIE

HARRY DIAMOND LABORATORIES
ATTN: SLCIS-IM-TI

U S ARMY ATMOSPHERIC SCIENCES LAB
ATTN: SLCAS-AE DR NILES
ATTN: SLCAS-AR DR H HOLT

U S ARMY COMMUNICATIONS R&D COMMAND
ATTN: AMSEL-RD-ESA

U S ARMY ENGINEER DIV HUNTSVILLE
ATTN: PRESTON J KISS

U S ARMY FOREIGN SCIENCE & TECH CTR
ATTN: AIFRTA

U S ARMY NUCLEAR & CHEMICAL AGENCY
ATTN: MONA-NU DR D BASH

U S ARMY NUCLEAR EFFECTS LABORATORY
ATTN: ATAA-PL
ATTN: ATAA-TDC
ATTN: ATRC-WCC LUIS DOMINGUEZ

U S ARMY SPACE & STRATEGIC DEFENSE CMD
ATTN: CSSD-GR-S W DICKINSON
ATTN: CSSD-TD W O DAVIES

U S ARMY STRATEGIC SPACE & DEFENSE CMD
ATTN: CSSD-H-LS B CARRUTH
ATTN: CSSD-SA
ATTN: CSSD-SA-E
ATTN: CSSD-SA-EV RON SMITH

USA SURVIVABILITY MANAGMENT OFFICE
ATTN: SLCSM-SE J BRAND

DEPARTMENT OF THE NAVY

NAVAL OCEAN SYSTEMS CENTER
ATTN: CODE 542 J FERGUSON

NAVAL RESEARCH LABORATORY
ATTN: CODE 2000 J BROWN
ATTN: CODE 2627
ATTN: CODE 4104 H HECKATHORN
ATTN: CODE 4183
ATTN: CODE 4700 S OSSAKOW
ATTN: CODE 4701
ATTN: CODE 4780 B RIPIN
ATTN: CODE 4780 DR P BERNHARDT
ATTN: CODE 4780 J HUBA
ATTN: CODE 4785 P RODRIGUEZ
ATTN: CODE 5300
ATTN: CODE 5326 G A ANDREWS
ATTN: CODE 5340 E MOKOLE
ATTN: CODE 8344 M KAPLAN
ATTN: JACOB GRUN CODE 4784

OFFICE OF NAVAL RESEARCH
ATTN: A TUCKER

DEPARTMENT OF THE AIR FORCE

AIR FORCE CTR FOR STUDIES & ANALYSIS
ATTN: AFSAA/SAKI

DNA-TR-92-98 (DL CONTINUED)

AIR FORCE ELECTRONIC WARFARE CENTER

ATTN: LT M MCNEELY
ATTN: SAVC
ATTN: SAZ

AIR FORCE PHILLIPS LABORATORY

ATTN: J KLOUSACHAR
ATTN: LAILA DZELZKALNS
ATTN: OP W BLUMBERG
ATTN: SANTI BASU

AIR FORCE SYSTEMS COMMAND

ATTN: DCS REQUIREMENTS J COLYER

AIR UNIVERSITY LIBRARY

ATTN: AUL-LSE

NATIONAL TEST FACILITY

ATTN: NTB/JPO DR C GIESE

PHILLIPS LABORATORY

ATTN: NTN

UNITED STATES STRATEGIC COMMAND

ATTN: J 533
ATTN: J 534
ATTN: J 614

DEPARTMENT OF ENERGY

EG&G, INC

ATTN: D WRIGHT

LAWRENCE LIVERMORE NATIONAL LAB

ATTN: L-97 T DONICH

LOS ALAMOS NATIONAL LABORATORY

ATTN: DAN WINSKE
ATTN: R W WHITAKER

SANDIA NATIONAL LABORATORIES

ATTN: D DAHLGREN 6410
ATTN: DIV 2344 ROBERT M AXLINE
ATTN: ORG 1231 J R LEE
ATTN: ORG 9110 G CABLE
ATTN: ORG 9110 W D BROWN
ATTN: TECH LIB 3141

OTHER GOVERNMENT

CENTRAL INTELLIGENCE AGENCY

ATTN: OSWR/NED
ATTN: OSWR/SSD L BERG

DEPARTMENT OF DEFENSE CONTRACTORS

AEROSPACE CORP

ATTN: BRIAN PURCELL
ATTN: C CREWS
ATTN: C RICE
ATTN: DR J M STRAUS
ATTN: G LIGHT
ATTN: J THACKER
ATTN: M ROLENZ

AUSTIN RESEARCH ASSOCIATES

ATTN: R THOMPSON

AUTOMETRIC, INC

ATTN: C LUCAS

BDM INTERNATIONAL INC

ATTN: W LARRY JOHNSON

BERKELEY RSCH ASSOCIATES, INC

ATTN: J WORKMAN
ATTN: N T GLADD
ATTN: S BRECHT

DELVIN SYSTEMS

ATTN: B PHILLIPS
ATTN: N CIANOS

DYNETICS, INC

ATTN: WILLIAM D TEPPER

ELECTROSPACE SYSTEMS, INC

ATTN: LINDA CALDWELL
ATTN: P PHILLIPS

EOS TECHNOLOGIES, INC

ATTN: B GABBARD
ATTN: R LELEVIER

GENERAL RESEARCH CORP INC

ATTN: J EOLL

GRUMMAN AEROSPACE CORP

ATTN: J DIGLIO

HARRIS CORPORATION

ATTN: E KNICK
ATTN: LYMUEL MCRAE

HORIZONS TECHNOLOGY, INC

ATTN: B LEE

INFORMATION SCIENCE, INC

ATTN: W DUDZIAK

INSTITUTE FOR DEFENSE ANALYSES

ATTN: E BAUER
ATTN: H WOLFHARD

JAYCOR

ATTN: J SPERLING

KAMAN SCIENCES CORP

ATTN: DASIAC
ATTN: E CONRAD
ATTN: G DITTBERNER

KAMAN SCIENCES CORPORATION

ATTN: B GAMBILL
ATTN: DASIAC
ATTN: R RUTHERFORD

LOCKHEED MISSILES & SPACE CO, INC

ATTN: J KUMER
ATTN: R SEARS

LOGICON R & D ASSOCIATES

ATTN: D CARLSON
ATTN: S WOODFORD

LOGICON R & D ASSOCIATES
ATTN: J WALTON

LOGICON R & D ASSOCIATES
ATTN: E HOYT

MAXWELL LABS, INC
ATTN: BILL RIX

MCDONNELL DOUGLAS CORP
ATTN: T CRANOR

MCDONNELL DOUGLAS CORPORATION
ATTN: R HALPRIN

MISSION RESEARCH CORP
ATTN: J KENNEALY
ATTN: R ARMSTRONG
ATTN: S DOWNER
ATTN: W WHITE

MISSION RESEARCH CORP
ATTN: R L BOGUSCH

MISSION RESEARCH CORP
ATTN: DAVE GUISE

MISSION RESEARCH CORP
ATTN: B R MILNER
ATTN: B SAWYER
ATTN: D KNEPP
ATTN: D LANDMAN
ATTN: F GUIGLIANO
ATTN: R BIGONI
2 CYS ATTN: R DANA
ATTN: R HENDRICK
ATTN: S GUTSCHE
ATTN: TECH LIBRARY

MITRE CORPORATION
ATTN: DR M R DRESP

MITRE CORPORATION
ATTN: G COMPARETTO

NORTHWEST RESEARCH ASSOC, INC
ATTN: E FREMOUW

PACIFIC-SIERRA RESEARCH CORP
ATTN: H BRODE
ATTN: R LUTOMIRSKI

PACIFIC-SIERRA RESEARCH CORP
ATTN: M ALLERDING

PHOTOMETRICS, INC
ATTN: I L KOFSKY

PHOTON RESEARCH ASSOCIATES
ATTN: D BURWELL

RJO ENTERPRISES/POET FAC
ATTN: STEVEN KRAMER

S-CUBED
ATTN: C NEEDHAM

SCIENCE APPLICATIONS INTL CORP
ATTN: C SMITH
ATTN: D SACHS
2 CYS ATTN: L LINSON

SCIENCE APPLICATIONS INTL CORP
ATTN: J COCKAYNE

SPARTA INC
ATTN: K COSNER

SPARTA INC
ATTN: D DEAN

SR! INTERNATIONAL
ATTN: R LIVINGSTON
ATTN: R T TSUNODA
ATTN: W CHESNUT

STEWART RADIANCE LABORATORY
ATTN: R HUPPI

TELEDYNE BROWN ENGINEERING
ATTN: J FORD
ATTN: J WOLFSBERGER JR
ATTN: N PASSINO
ATTN: RONALD E LEWIS

TOYON RESEARCH CORP
ATTN: J ISE

TRW SPACE & DEFENSE SECTOR
ATTN: D M LAYTON
ATTN: HL DEPT LIBRARY

VISIDYNE, INC
ATTN: J CARPENTER
ATTN: J DEVORE
ATTN: J THOMPSON
ATTN: W SCHLUETER